Ultrafiltration of a surfactant using chemically modified ceramic-zeolite composite membranes

A thesis submitted
in partial fulfillment of the requirements
for the degree of
Master of Technology

By
ASHWIN POTDAR

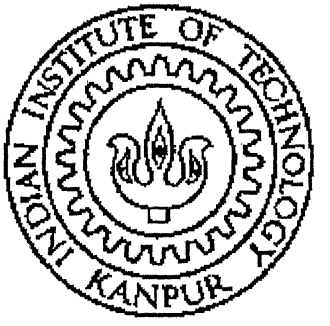

To the
DEPARTMENT OF CHEMICAL ENGINEERING
INDIAN INSTITUTE OF TECHNOLOGY, KANPUR
January 2001

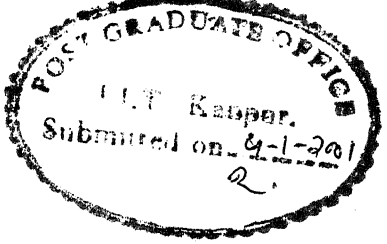

CERTIFICATE

This is to certify that the thesis entitled **"Ultrafiltration of surfactant using chemically modified ceramic-zeolite composite membranes"** is the original work of Mr. Ashwin M. Potdar carried out under my supervision, and has not been submitted elsewhere for a degree.

(Anil Kumar)
Professor
Department of Chemical Engineering
Indian Institute of Technology
Kanpur-208016, India.

ABSTRACT

Ceramic-zeolite composite membranes have been synthesized by growing a zeolite layer hydrothermally over mesoporous ceramic clay supports via in-situ crystallization. The latter have been prepared by using a standard clay mixture followed by coating with a thin mesoporous film of kaolin by slip casting. Using the XRD analysis, these ceramic-zeolite membranes have been characterized with respect to their molecular structure (Nepheline Hydrate) and geometry of the crystal lattice (Orthorhombic). These zeolite membranes have been chemically modified using NO_X gas at 225^0C and the $-NO_2$ group bound to the silicon (Si) atom of the support can further be reduced to an amine group ($-NH_2$) by reaction with hydrazine hydrate. These unmodified and modified zeolite membranes have also been characterized for their pore size and pore size distribution using the Bubble point technique and is seen to be in the range of 273-156 A^0 for unmodified membrane. This chemical modification technique does not lead to pore blocking and causes a small decrease (32%) in pore size from 273-156 A^0 to 181-109 A^0. The XRD studies of the modified and unmodified zeolite membrane show that the crystal structure of the zeolite deposited changes from orthorhombic (98.27% crystalline) for the unmodified zeolite to tetragonal (82% crystalline) for the modified zeolite. We have also calculated the theoretical exchange capacity of the modified zeolite membranes to be 0.8 meq/dry mass. We have found that the anion exchangeability of this modified zeolite membrane increases with the silica content of the zeolite layer. The ultra filtration experiments have been carried out using these unmodified and modified zeolite membranes, involving a surfactant, Cetyl pyridinium chloride (CPC). We have found out that the rejection capacity of the membrane increases at least three folds, after chemical modification, indicating the improvement in the surface properties. After modification of these zeolite membranes, the ratio of surfactant to water flux increases, which confirms their hydrophilicity.

Acknowledgements

I feel pleasure in expressing a deep sense of gratitude to **Prof. Anil Kumar**, my thesis supervisor and mentor. Constructive criticism, valuable guidance and constant encouragement by him have gone a long way in shaping this work. His clear deep insight into my problems, encountered during the period of my work enabled me to accomplish the task. His friendly nature and ever helping attitude always made me feel at home at I.I.T Kanpur.

I am grateful to other faculty members of the Chemical Engineering Department at IIT Kanpur for the invaluable suggestions and guidance provided by them from time to time.

I express my special thanks to all the staff members of Chemical Engineering Department and ACMS for the cooperation extended by them.

Thanks are due to my labmates **Shankhanilay**, **Anupam**, **Roshan**, **Pankaj**, **Manish**, **Mishraji** and **Neelkandan** for maintaining a collegial, cheerful, and cooperative atmosphere, thus making the lab a perfect workplace.

Inspite of all my diligence and efforts, it was not possible for me to complete this thesis report without the moral support and help of my dear friend **Raju**. Special thanks to him for being supportive at the time of need and being always affectionate.

Finally, I express my sincere thanks to all my friends for their splendid company and unforgettable cooperation during my stay at I.I.T Kanpur and making it the most memorable one.

(Ashwin Potdar)

Contents

List of figures

List of Tables

CHAPTER 1

INTRODUCTION

Membrane separation processes are used in wide range of applications and these applications are growing continuously[1]. The classification of the membrane processes is based on the following:

1) The nature of the membrane i.e. natural or synthetic material
2) The structure of the membrane i.e. porous or nonporous
3) The application of the membrane i.e. gas separation, liquid-liquid separation etc

A membrane separation process requires two bulk phases physically separated by a membrane interphase. Due to difference in physical and chemical properties between the membrane and the permeating components, transport of one component through the membrane occurs more readily than the other. The driving force in this class of separation could be an external pressure, chemical potential or concentration difference. Industrial applications of asymmetric inorganic ceramic membranes have been developed[2] which consist of an ultra thin dense top layer supported on a porous inorganic sub layer.

Ceramic membranes are important class of inorganic composite membranes. Recently, the use of ceramic membranes in separations has increased since they offer number of advantages over organic polymer membranes. Because of their advantages, the areas of application of ceramic membranes are growing and Table 1.1 lists some of these along with the areas of application[3-9]. The thermal inertness of the membrane readily permits long-term operation at elevated temperatures. It has tubular pores, which are less susceptible to fouling. As a result of this, it can be readily cleaned compared to the organic polymeric membranes.

Ceramic membrane supports have two types of geometries, tubular and flat-disk[10]. The tubular supports used are generally made of α-alumina, while flat supports are porous disks made of ceramic materials like α-alumina, zirconia, clay etc. Most of these ceramic disks and tubular supports are commercially available, although they can be synthesized using ceramic raw materials as reported in reference 11. During

synthesis of the supports, sintering is an important step, which condenses the clay particles into a crystalline, hard, and rigid material. Drying of the compacts should be carefully controlled to avoid shrinkage and warping.

Ceramic membranes come under the class of composite membranes and they consist of two main layers, the bulk inorganic support layer and the thin dense separating layer. The separating layers are synthesized using the sol-gel technique in which a thin layer of the material, having the separation properties, is deposited on the bulk porous support. A variety of materials like α-alumina, γ-alumina, TiO_2, micro porous glass, ZrO_2 and zeolites have successfully been deposited on top of bulk supports[12, 13]. The separating layer of zeolites has following advantages over other above-mentioned materials, when used as membranes.

1) The pore size of the membrane can be adjusted by choosing the appropriate zeolite. For example, small-pore (A-type)[14-17], medium-pore (MFI- and FER-type)[18-24] and large-pore (MOR- and Y-type)[25,26] zeolite membranes have been prepared.
2) The hydrophilic/hydrophobic nature of the membrane can be modified by introducing different functional groups on the zeolite framework[27].
3) The catalytic properties of the zeolites can be used for the catalytic membrane reactors[28].
4) As zeolite is resistant to high temperatures (<600°C), the films can be used under conditions of high temperature and pressure, where it is difficult to use the organic polymer membranes. It becomes possible to separate mixtures at a molecular level, under severe conditions[29].
5) Zeolites contain well-defined cavities and channels of molecular dimensions[30]. These cavities and channels are more or less uniform in size. Because of their unique pore structure, a sharp pore size distribution can be achieved within the inorganic separating layer.

Zeolites are micro porous inorganic crystalline polymers, which can accept molecules of certain size and reject molecules of larger dimensions. These molecular sieving properties of the zeolite powder can be converted into a membrane configuration[31].

For synthesizing a zeolite membrane, the zeolite crystals must grow in an interlocking fashion to form a continuous layer on a porous substrate. This layer must be mechanically stable and it should also provide good flux. Geus et.al[32] and Bakker et.al[33]

studied the growth of zeolite films on various porous substrates including α-alumina, zirconia, clay and sintered steel-wool composites. One of the major findings of these works was that the substrate surface plays an important role in determining the type of zeolite film grown. For example, analcime zeolite grew on α-alumina and ZSM-5 grew on clay, while a mixture of analcime and ZSM-5 grew on a ZrO2-α alumina composite. Various types of zeolites like MFI, FER, MOR, Y-type, A-type, silicoaluminophosphates (SAPO)[33,34,35], ZSM-5 and ZSM-35 have been reported as separating layers over inorganic and ceramic supports.

Zeolite membranes, with molecular sieving properties, can be prepared by several methods and some of these are listed below.

1) By hydrothermal synthesis[19,36]
2) By growing zeolites on metal or alloy surfaces[37-39]
3) By the vapor phase transport method[19, 25,40,41]
4) By using organic solvents[42, 43].

In most of the cases, zeolitic membranes are generally obtained by hydrothermal synthesis and the synthesis gel composition is similar to that used by Grose and Flanigen[35]. It consists of a silica source, an alumina source and an alkali (usually NaOH) in presence of a surfactant. In the hydrothermal synthesis, zeolites are grown over the porous supports via in-situ synthesis under pressure. Surfactant present is used as a structure-directing agent. These surfactant molecules aggregate themselves to form miscelles and these miscelles interact with the organic molecules by completely combining them within it. This leads to the formation of inorganic mesopores[36] within the ceramic membranes. After the reaction, the resulting membrane is calcined during which the surfactant molecules, in the miscelles, are burnt leaving behind an open-pore framework.

Davis et.al[38] and Wenyang et.al[39] reported the growth of zeolites over metal and alloy surfaces. Tsikoyannis and Haag[40] studied the formation of ZSM-5 zeolite layers on a variety of flat, nonporous surfaces like silver, steel and Teflon. They observed that the crystal layers formed on metals were firmly bonded to the substrate but the layer formed on Teflon could be easily peeled off.

Relatively recent method of zeolite synthesis through vapor phase transport has been reported. Dong et.al[40] reported the first synthesis of zeolites ZSM-5 and ZSM-35 over glassy plates by the vapor phase method. The vapors of diethyl amine, ethylenediamine and a mixture of ethylenediamine-triethlyamine were used to obtain zeolite ZSM-5. Matsukata et.al[25] synthesized a large-pore MOR zeolite as a membrane by the vapor phase transport method. In this method, aluminosilicate dry gels are converted into zeolites under the vapors of organic templating agents and water. FER zeolite membrane[41] and a mixture of MFI and FER zeolite[41] have also been synthesized by this technique. Many types of high-silica zeolites like ZSM-5[42], ZSM-35[42], silicalite-1[43], ZSM-39[43] and ZSM-48[44] have also been synthesized from the organic solvents like ethylene glycol and propanol. After synthesis, the zeolites are separated from the organic solvent phase by filtration or centrifugation. These zeolites are then used in membrane form by deposition on a support.

Recent zeolite membrane preparations have all involved ZSM-5 zeolite. Jia et.ai[45] used macro porous α-alumina tubes as supports coated on the inside by a mesoporous γ-alumina layer. The tubes were filled with a synthesis gel and placed in an autoclave at 180°C. After about 12 hours of heating, a zeolite layer was formed on the γ-alumina surface. In a different preparation scheme employed by Xiang and Ma[46,47], silicalite/ZSM-5 membranes are prepared as follows. A porous α-alumina tube or disk is loaded with the synthesis gel and brought in contact with water vapor at 130-200°C under pressure. Jia et.al[48] and Vroon[49] synthesized silicalite layers on ceramic disks and used SEM and XRD to confirm that a continuous silicalite thin layer was formed on the surface. Falconer et.al[50] reported the synthesis of alkali-free H-ZSM5 membranes by in-situ crystallization on porous α-alumina, γ-alumina and stainless steel supports. These membranes were prepared from different silica sources and they were characterized by XRD, SEM and electron probe microanalysis. In all these cases, the synthesis was done by contacting the support with the synthesis gel but composition and orientation of the support varied in different preparations. Yan et.al[51] reported that the choice of synthesis solution is critical for preparing good qùality membranes. They suggested that some compositions give a continuous layer of zeolite crystals while some other compositions gave isolated zeolite crystal patches with some of the surface remaining vacant.

The pore sizes of the ceramic membranes have to be controlled for various ultra filtration and micro filtration applications. These methods discussed above achieved only the reduction of the pore size by the deposition of zeolites, without any change in the surface properties. However the chemical properties of the membrane surfaces are important for separation applications. Thus, the necessity of modification of the membrane arises which is done to achieve the following two goals.

1) To alter the pore size of the ceramic support
2) To change the chemical properties of the membrane surfaces i.e. to increase its hydrophilicity.

These properties, in zeolitic membranes, are modified by the following two techniques.

1) Entrapment of inorganic metal oxides or organic molecules during the sol-gel reactions
2) Chemical reactions with silica atoms in the matrices

In the first method, organic or inorganic groups are introduced into the pores of a porous ceramic membrane. After the sol-gel reaction, these chemical compounds are trapped inside the membrane matrix and this is normally achieved through Chemical vapor deposition (CVD) and Chemical vapor infiltration (CVI). In the CVD method, counter diffusion of vapors of two substances occurs in the membrane pores and a solid product is deposited on the pore surface[51-53]. In the chemical vapor infiltration (CVI) method, a vapor is introduced from one of the membrane surfaces into the membrane pores and it is deposited, after a chemical reaction, on the membrane pore surfaces[54-56]. In the liquid phase approach, a small amount of solution containing a solid is sucked into the membrane pores by capillary force. The solid remains on the pore surface after the solvent has dried[57, 58]. Lin and Burgraaf[57] reported the increase in pore size of the membrane after CVD. They showed that the pore size of γ-alumina membranes, having a pore diameter of about 4nm, could be increased to the range of 4-100nm by a proper heat treatment method. Uhlhorn et.al[58] developed a reservoir method for modifying porous γ-alumina thin films supported on a larger pore α-alumina layer. In this method, drying of the solvent takes place only on the surface of the γ-alumina film. CVD of γ-alumina membranes greatly improved their thermal stability and the catalytic properties[57-59]. Various methods have been reported to alter the pore size of zeolite

materials[60] and in one method, the pore opening of zeolite ZSM-5 has been reduced by CVD of thin silica layer on the external surface of the zeolite crystals[61]. Table 1.2 summarizes some of the studies on the modification of porous ceramic membranes[52-63].

In most of these modification methods, a solid metal oxide has been deposited inside the membrane pores. However, these methods have the disadvantages of blocking the pores as well as reducing the pore diameters leading to decrease in flux. Table 1.2 gives examples for trapping inorganic molecules, but one can similarly trap organic molecules as shown in the following recent references. Chaufer et.al[64] coated tubular zirconium oxide (ZrO_2) membranes with polyethyleneimine followed by further cross-linking with diglycidylether of bisphenol A. To change the net charge, this polymer coating was chemically grafted with carboxylate moieties. Guizard et.al[65] reported the CVD of inorganic membranes with heteropolysiloxanes and the chemical composition was varied by introducing methyl groups into the modified silica network. This was done to change the hydrophobic behavior of the membranes. While vast literature is available on entrapping different molecules in the ceramic matrices, only one technique is known in which the silica molecule of the ceramic reacted. In this, different organosilanes (for example, triethoxy amino propyl silane) are reacted with the ceramic support. However literature shows that these reactions are liquid phase leading to pore blocking and substantial reduction of pore size.

In the present work, we have developed a new gas phase chemical modification of the silica matrix of ceramic support as well as the zeolite-separating layer of the membrane. The modification is carried out by gas phase nitration using a mixture of NO and NO_2 (called NO_X). This scheme introduces the nitro group ($-NO_2$) in the zeolite separating layer and the silica matrix, which can subsequently be reduced to an amine group ($-NH_2$) using hydrazine hydrate. The advantage of amine modification of ceramics lies in the fact that these groups can ionize and impart charge to the material. This is in addition to converting the membrane into a hydrophilic material. The amine groups are highly reactive and can further react with various other organic materials. In this gas phase chemical modification using NO_X, the strength of the membrane remains unaffected and the pore blockage occurs negligibly. Moreover, the hydrophilic nature of the membrane surface results in an increase in the water flux. We have first prepared macroporous ceramic clay supports by using a standard clay mixture followed by coating

them with a thin mesoporous kaolin film via slip casting. The zeolite-separating layer has been deposited on the above clay supports hydro thermally via in-situ synthesis. The organic template ions (tetrapropyl ammonium) are removed on calcination at 400°C in air. After calcination, zeolite films are stable and these films have been confirmed using the standard XRD technique and SEM. The average pore size and the pore size distribution of the membrane have been determined using the bubble point technique, which works on the principle of displacement of a wetting liquid. The bubble point experiments show that after every modification step, there is a marginal decrease in the pore size and the pore size distribution is slightly narrowed. Ultra filtration experiments have been performed using high molecular weight surfactants like Cetyl pyridinium chloride (CPC). These experiments show that the rejection capacity of the membrane increases for the surfactant solution (CPC in water) at least three folds due to the chemical modification.

Table 1.1

Advantages and applications of Ceramic Membranes

Advantages	Application Area
High thermal stability	High temperature gas separation[3], steam cleaning of the membrane in food, pharmaceutical, dairy and beverage industry to avoid contamination[4]
High structural stability and less degradation. Resistant to abrasion	Milk separation, sterilization of liquids in pharmaceutical industry[5]
Ability to withstand prolonged exposure to organic solvents	Heavy hydrocarbon separations, deasphalting of residual oils[6]
Chemical stability over a wide pH range	Separations of feeds with alkaline pH hot caustic or acid cleaning
Less susceptible to fouling	Processing of industrial waste[7-9], colloidal ash removal from coal liquids

- **There are certain disadvantages of ceramic membranes like high initial cost and brittleness.**

Table 1.2

Studies on the modification of ceramic membranes

Investigators	Membranes Modified	Method of modification
Miller and Koros[56]	Supported γ-alumina membranes	Chemical deposition of TDFS (organometallic)
Liu et.al[63]	Supported γ-alumina membranes	CVD of SiO_2 and organic vapor deposition of carbon
Kitao and Asaeda[52]	Supported silica membranes prepared by the sol-gel method.	CVD of SiO_2 from SiH_4 vapor and O_2
Lin et.al[62]	One-layer γ-alumina membranes, two-layer zirconia membranes	CVD of Y_2O_3/ZrO_2 from $YCl_3/ZrCl_4$ and H_2O vapors
Lin and Burggraaf[53]	One-layer alumina membranes and La-modified supported γ-alumina membranes	CVD of ZrO_2 from chloride and H_2O vapors.
Uhlhorn et.al[58]	Supported γ-alumina membranes	Deposition of Ag, MgO and V_2O_5 by the reservoir method
Okubo and Inoue[55]	One-layer porous glass membranes	Deposition of SiO_2 from TEOS vapor
Ma et.al[59]	Supported γ-alumina membranes	Wet-impregnation of Fe_2O_3 and Al_2O_3

CHAPTER 2

Experimental section

The ceramic-zeolite composite membranes could be prepared by following steps as given below.

2.1 Preparation of Porous clay supports.

The clay supports are prepared from a standard clay mixture consisting of the composition given in Table 2.1

These clays, needed for the synthesis of the supports, are collected locally from S. N. Pandey and Co., Nayaganj, Kanpur. Table 2.2[66] gives the chemical formula and the density of each clay raw material. The clay mixture is prepared first in the composition given in Table 2.1 followed by adding distilled water. The mixture is mixed thoroughly and the clay suspension is poured into shallow metal (aluminium) rings (diameter 66mm; height 4mm) placed on a gypsum surface. The metal rings are carefully removed and the clay compacts are dried overnight under ambient conditions. The drying is continued by placing the compacts in an oven at 100^0C for 24 hrs followed by further drying at 250^0C for another 24 hrs. This drying at elevated temperatures ensures the complete removal of moisture from the clay compacts. Controlled and slow drying avoids the formation of cracks on the clay surface. During the drying process, the clay compacts are placed vertically over grooves cut on insulating firebrick surfaces, so that maximum area of the compacts comes in contact with the hot air. This ensures even and uniform drying from all the sides.

After through drying, the clay compacts are transferred into a furnace for sintering at 900^0C for 8-10 hrs. During the process, the clay compacts condense into a hard and rigid, crystalline material that is porous in nature. Again the compacts are placed vertically in the furnace so that all the sides are uniformly sintered. After sintering, the clay supports are polished on silicon carbide abrasive paper (No. C-220) to get smooth, flat clay disks. This

polishing from 4mm thickness to 2-3mm eliminates any warping produced on the surface during the sintering process.

2.2 Slipcasting of the clay support.

The clay supports, prepared by the above method, are macroporous in nature. Slipcasting is done to change the macroporous nature of the support by coating it with a thin mesoporous film. For this purpose, a suspension of Kaolin is prepared (50 wt.% in water) and the supports are dipped in this. A thin layer of Kaolin is deposited on the compact after the sol fills all the pores. Then it is dried in an oven at 100^0C for 24 hrs. The result supports are subsequently sintered at 900^0C for 8 hrs. During this second stage sintering, the Kaolin deposited on the surface and inside the pores of the compact condenses into a hard material resulting in a mesoporous support. Weight of the supports is taken before and after Slipcasting and a weight gain is observed indicating the deposition of a mesoporous layer inside the pores. The clay supports, thus prepared are used for the zeolite synthesis reaction. The pore sizes of these slipcast supports are determined by the Bubble point technique, which is described later.

2.3 Synthesis of ceramic-zeolite composite membrane

Zeolite films are grown hydrothermally on the above mesoporous clay supports with a standard synthesis mixture. To 100 ml of distilled water, 3.96 g. Quartz (SiO_2), 1.682 g. Al_2O_3, 4.26 g. NaOH and 13.3 Tetrapropyl ammonium bromide (TPAB) are added and the mixture is stirred vigorously for 5-10 minutes[11]. The molar composition of the liquid mixture prepared is 200 SiO_2: 50 Al_2O_3: 160 Na_2O: 150 TPAB: 16666 H_2O. The clay supports are placed at the bottom of a stainless steel Parr 1litre autoclave and the synthesis mixture is poured over it. The reactor is set at 180^0C, 150 psi and the mixture is subjected to hydrothermal crystallization for 2-5 days. After the hydrothermal reaction, the disks are washed with water and dried in an oven at 100^0C overnight. The zeolite-clay composites are calcined at 400^0C for atleast 10 hrs. In calcination, the heating rate is carefully controlled, during which the organic surfactant ion (TPAB) is burnt leaving an

open pore zeolite framework on the clay substrate. Table 2.2 shows the optimal conditions and the molar composition of the solution for the synthesis of zeolite films. Gain in weight of the clay supports before and after the hydrothermal reaction is noted.

2.4 Characterization of ceramic-zeolite composite membrane.

The ceramic-zeolite membranes, synthesized this way are characterized with respect to the following.

1. X-ray Diffraction Pattern (XRD)
2. Scanning Election Microscopy (SEM)
3. Pore diameter and Pore size distribution using the Bubble point technique.

2.4.1 X-Ray Diffraction Pattern (XRD)

XRD analysis is employed to monitor zeolite layer formation over clay support using X-Ray power Diffractometer, which uses the X-Ray source CuKα, (Model Isodevyeflux 2002, Rich Seifert & Co., West Germany). During all XRD analysis, the X-Ray wavelength is kept constant at 1.5406 ^{0}A and the relative intensity of the diffraction is recorded as the function of 2θ. The d-spacing value of standard aluminosilicate zeolite sample reported in JCPDS file is used as the basis of the comparison, as described later.

2.4.2 Scanning Electron Microscopy (SEM)

The structural morphology of the zeolite layer grown on the porous clay supports has been examined by Joel-840-A scanning electron microscope (SEM).

2.4.3 Pore size determination using the Bubble point technique

The Bubble point technique is used to determine the average pore size and the pore size distribution of the zeolite membrane. Various methods are available for determining this

such as nitrogen adsorption–desorption[67, 68] and mercury penetration[69]. But these methods are unsatisfactory for asymmetric ceramic membranes due to the following reasons.

1. They cannot distinguish between dead-end pores and pores available for permeation.
2. They cannot differentiate between the pores of the thin separation layer and the bulk support.

The Bubble point technique[70] is an easy, fast and inexpensive method, which determines the maximum pore size and the pore size distribution of the ceramic membrane. This technique is based on the principle of displacement of a wetting liquid. The membrane is wetted with a liquid, which is held in the pores by capillary forces. Another fluid (liquid or gas), acts at increased pressure on the one side of the membrane and displaces the former. The pressure difference Δp needed to drive away the former liquid from a pore with radius r is given by Laplace's equation

$$\Delta p = \frac{2\sigma \cos\theta}{r} \qquad (2.4.3)$$

Where, σ is surface tension of the two fluids system and θ is the angle of contact between the wetting liquid and the solid (support)

The Bubble point technique is carried out in an experimental setup shown in Fig 2.1. The setup consists of a stainless-steel tubular cell with the material of construction as SS316, volume of the cell as 1000 ml, its diameter and height as 76 mm and 24cm respectively. This cell is placed over a SS base plate, which houses the membrane. The membrane is prepared for the Bubble point technique by first drying in an oven at 100^0C for 10 hours to remove any adsorbed contaminants. The dry membrane is placed in a perforated aluminum casing, which is used to provide support to the membrane. This casing withstands the pressure of the cell and the O-rings and this way the breaking of the fragile and brittle ceramic membrane is completely eliminated. For this, the diameter of the ceramic membrane is reduced by filing, until it fits inside the aluminum casing. The clearance between the outer edge of the membrane and the ID of the casing is sealed with the help of a fast-setting epoxy resin. The epoxy is allowed to set overnight after which it

becomes hard and completely waterproof. This membrane housing is placed in the base plate and the cell is placed over it with rubber O-ring between them. The specifications of the final membrane and the aluminium casing are given in Table 2.3.

The whole assembly is connected to a nitrogen cylinder (150-psi), which provides the pressure for the process, through high-pressure rubber tubing. The water-butanol wetting-nonwetting system is chosen for this process because of their wide range of surface tensions. The contact angle for the silica-butanol-water system is determined to be 58.5^0 by using a Wilhelmy balance[70].

First, the cell is filled with water and small amount of pressure is applied. The water drips through the membrane pores and after some time the pores get filled with the wetting liquid completely. After the water is drained out, the cell is filled with the non-wetting liquid, butanol. The pressure is increased gradually until at a particular value, butanol displaces the water present in the pores. At this pressure, the flow rate of butanol is noted. After the butanol is drained out, the membrane is brought in contact with water once again and the pressure is applied till the liquid fills in the pores. After the water is removed, butanol is again filled in the cell and the procedure is repeated by alternately changing the wetting and non-wetting liquids. The pressure is increased successively and the resulting butanol and water flow rates are recorded. The data is tabulated and equation (2.4.3) is used to determine the maximum pore size and the pore size distribution of the membrane. The flow rates of water and butanol are plotted as a function of pressure difference (Δp). This method is also used to determine the pore size distribution of modified membranes.

2.5 Gas phase nitration of ceramic-zeolite composite membrane using NO_X.

Direct gas phase nitration of the zeolite-separating layer as well as the clay support is carried out in a three-litre reaction bottle shown in figure 2.2. The lid of the reaction vessel is made-up of stainless steel and is equipped with a brass cap with 1.2 mm opening at the top for injecting the gas, which is sealed by a silicon rubber septum. Double neck round bottom flask is used to produce NO_X by reacting sodium nitrate $NaNO_2$ (10 g mole)

with sulfuric acid (98% H_2SO_4, sp. gr. 1.98, 25 ml) and ferrous sulfate $FeSO_4$ (1gmole). One neck of the flask is closed with rubber septum for withdrawing gas with a 50 ml syringe. The generation of NO_X occurs through the following mechanism.

$$2NaNO_2 + H_2SO_4 \rightarrow Na_2SO_4 + 2HNO_2 \qquad \rightarrow 2.5.1$$

$$3HNO_2 \rightarrow H_2O + HNO_3 + 2NO \qquad \rightarrow 2.5.2$$

$$FeSO_4 + NO \rightarrow (Fe, NO)\ SO_4 \qquad \rightarrow 2.5.3$$

$$2NO + O_2 \rightarrow 2NO_2 \qquad \rightarrow 2.4.4$$

The ceramic-zeolite membrane is taken in the reaction vessel. The vacuum is created inside it by a vacuum pump and its value should be such that when NO_x gas is introduced into the reaction bottle, at the reaction temperature, the total pressure should not exceed the atmospheric pressure to avoid leakage. Around 500 ml of NO_x is introduced in the bottle, every run. The nitration reaction in a single run is carried out at 225^0C in an oven for about 18 hours. Then the reaction vessel is cooled and water formed in reaction, which is found to adhere to the wall of the vessel, is cleaned. This reaction is repeated till the membrane becomes equilibrated for any more reaction with NO_x. The membrane is now ready for the amination reaction. Small part of the nitrated membrane if required is broken for characterization. Approximately 4 runs i.e. 2000 cc of NO_x is employed for one membrane sample. After every run, the gain in weight of the membrane is noted.

2.6 Amination of Nitrated zeolite membrane

Amination of the nitrated membrane is carried out with hydrazine hydrate. The nitrated membrane is placed at the bottom of a beaker and about 100 ml of 50 % Hydrazine Hydrate is poured over it and the mouth of the beaker is covered with an Aluminium foil to prevent escape of the vapors produced during amination. The membrane sample is refluxed for 4-5 hrs at 65^0Cin a water bath, which is maintained at 70^0C. After the reaction, the membrane is washed thoroughly with distilled water and dried in an oven at 100^0C. This

aminated zeolite membrane is ready for the bubble point test and the ultrafiltration experiments. A small part of the membrane is broken, if required, for its characterization. The membrane now has amine groups attached and can exchange chloride ions. The anion exchange capacity of the aminated zeolite membrane is found out by standard procedure described in section 2.7.

2.7 Determination of Anion exchange capacity of the zeolite membrane

The exchange capacity of aminated zeolite membrane is determined using gravimetric method given in ASTM standard number ASTMP (2187, 2687, 3087, 3375 and ISI). It involves the following two steps

2.7.1 Regeneration of Anion

In this method, first mixed acid is prepared by mixing 18.1 ml of H_2SO_4 (sp. gr. 1.84) with 27.5 ml of HCl (sp. gr. 1.19) in 500 ml of distilled water. The entire contents are made up to 1000 ml using distilled water. After this, the test water is prepared by diluting the mixed acid by distilled water up to 1 percent concentration. This test water is then added to the modified zeolite membrane is a quantity of 100 ml per gram of the weight of the membrane and kept for 24 hrs. Then, the membrane is removed and washed with distilled water till the filtrate becomes free from any acidity as checked by pH meter.

2.7.2 Anion capacity determination

The anion regenerated modified membrane is kept in 0.1 N $NaNO_3$ solution (0.85 gms in 100 ml) for 24 hrs. The membrane is then removed and approximately 1.7g $AgNO_3$ is added to the filtrate and 2-3 drops of concentrated HNO_3 is added to bring the pH of the solution to about 2.0. The entire mass is again kept for 24 hrs and the chloride ion present in the filtrate forms AgCl, which appears as a white precipitate. The precipitate is filtered

and weighed and the anion exchange capacity of modified zeolite membrane is calculated using the following relation.

Anion exchange capacity (Meq/gm) = W_1 / MW_2

Where W_1 is the oven dry mass of silver chloride precipitate, M, Molecular weight of silver chloride and W_2 is the mass of dry membrane.

2.8 Permeate Flux and Rejection in Ultrafiltration

The water flux through a ultrafiltration membrane can be described by Darcy's law[71] for flow through porous media. It states that the volumetric flux is directly proportional to the applied pressure gradient.

$$J_w = K\Delta p_{app} \qquad (2.8a)$$

$$K = 1 / R_m \mu_w \qquad (2.8b)$$

Where,

$R_m \rightarrow$ intrinsic hydraulic resistance of the membrane

$J_w \rightarrow$ water flux

$\mu_w \rightarrow$ viscosity of water

In membrane separation, the membrane rejection for a given solute is usually characterized by rejection coefficient. The solute rejection is defined as

$$R_{sol}\,(\%) = 100\,x\left(1-\frac{C_P^{\,sol}}{C_R^{\,sol}}\right) \qquad (2.8c)$$

Where,

C_P^{sol} = solute concentration in Permeate

C_R^{sol} = solute concentration in Retentate

This rejection corresponds to the observed rejection based on the bulk retentate concentrations. If the rejection is based on retentate concentrations at the membrane surface, then it is referred to as intrinsic rejection.

$$R_{int}(\%) = 100 \times \left(1 - \frac{C_P^{sol}}{C_m^{sol}}\right) \qquad (2.8d)$$

C_m^{sol} = Solute concentration at the membrane surface.

In the present study, we have subjected the modified membrane to the ultrafiltration experiments.

2.9 Ultrafiltration experiments

The ultrafiltration setup is the same as shown in fig 2.1. For the separation purposes, the membrane is placed in the aluminum casing as described in section 2.4.3. A high molecular weight cationic surfactant, cetylpyridinium chloride (CPC) is chosen for the ultrafiltration experiments. During the experiment around 600 ml of an aqueous surfactant solution (2 wt% CPC) is first added in the cell over the membrane housing. The cell is then sealed, and nitrogen pressure is applied to start the flow through the membrane. Surfactant flowing through the membrane is collected and its flow rate is determined at regular intervals. This is continued until the steady state flow rate is achieved. The permeate and the retentate are collected separately and the cationic surfactant concentrations are determined by a conductivity meter (DDR conductivity meter, power 230V, range 0-200 mMhos and cell constant 0.9-1.1). The conductivity meter is calibrated before hand by using 0.1 N KCl and the CPC solutions of known concentrations. The ultrafiltration experiments are repeated at different pressure readings. At various pressures, the flux and surfactant rejection values are calculated. The rejection of the surfactant is plotted as a function of the applied pressure.

2.10 Synthesis of Mesoporous silica layer over Porous clay supports

We have also synthesized mesoporous silica films over clay supports starting from tetraethylorthosilicate (TEOS) by using the following procedure. To 100 ml of water, 15 gms of HCl, 2.3147 gms TEOS and 2.188 gms of cetyltrimethylammonium bromide (CTAB) are added and the mixture is stirred vigorously for 10 minutes[72]. The molar composition of the liquid mixture prepared is 100 H_2O: 7.4 HCl: 0.11 CTAB: 0.2 TEOS. Here CTAB is the cationic surfactant, which is used as a structure-directing agent, and TEOS is the silica source reagent. The resulting mixture is poured over clay supports placed at the bottom of the autoclave and the crystallization is carried out in the same manner as described in section 2.3. But, in this case, the temperature is controlled at 80^0C and the duration of the reaction varies from 1-2 hr to 1 week. After about 2 days, the compact disks are washed thoroughly, dried and calcined at 500^0C in air for 4 hrs. Table 2.3 shows the molar composition of the solution and the optimal conditions used for the synthesis of mesoporous silica layer.

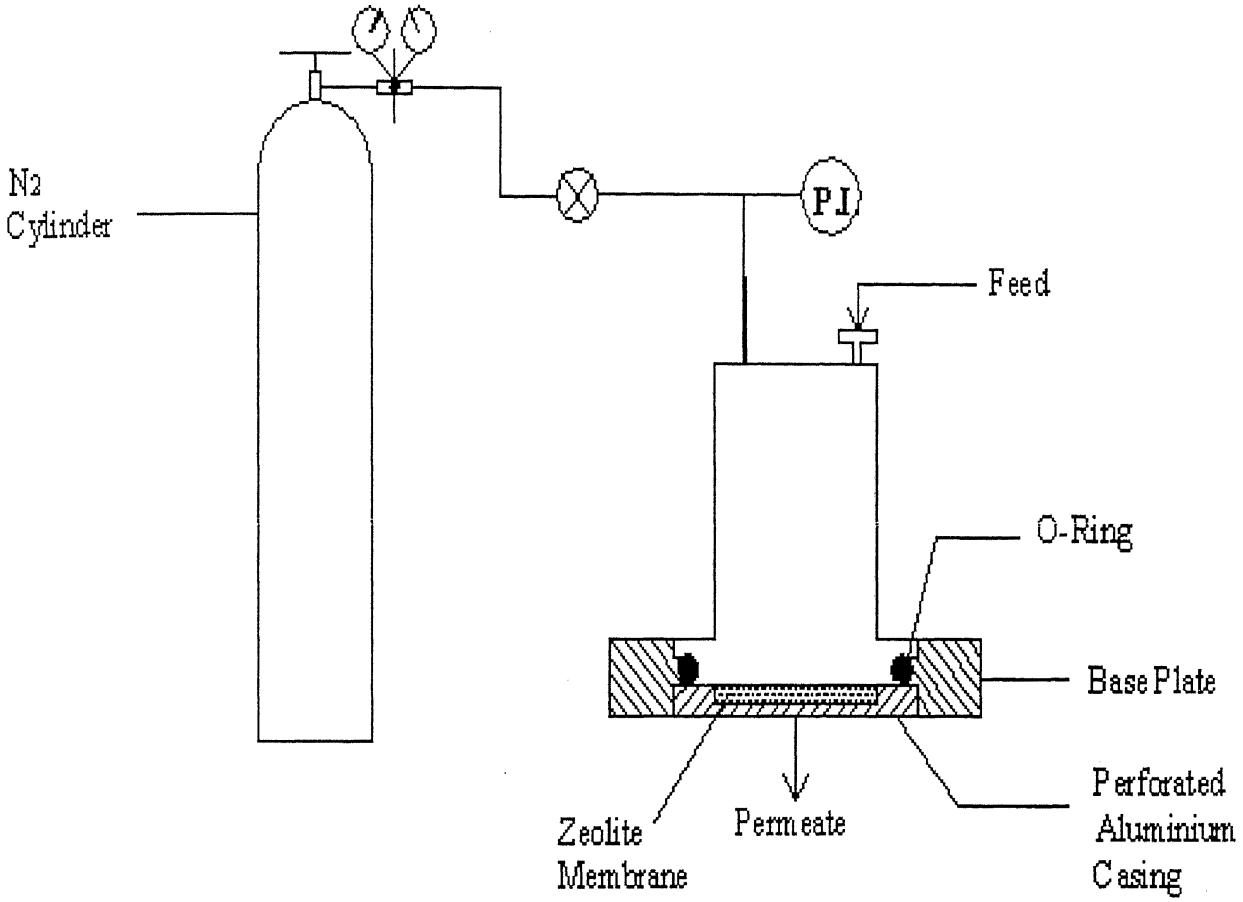

Fig 2.1: Experimental setup for the Bubble point technique

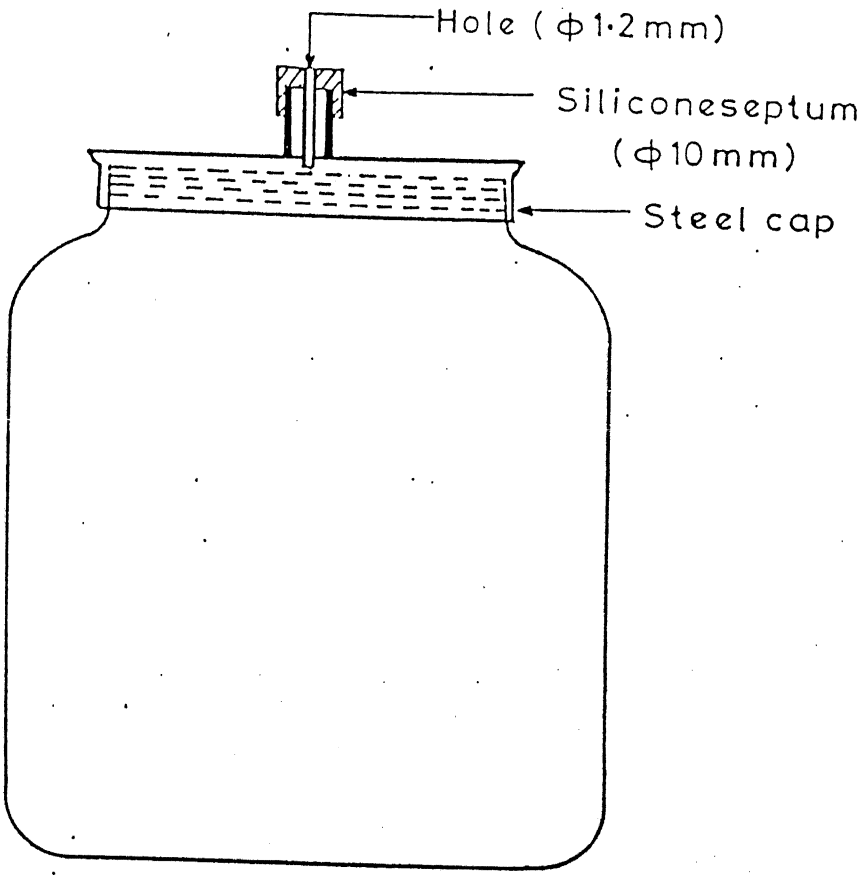

Fig 2.2: Reactor used for the nitration of zeolite membranes

Table 2.1

Chemical Formula and density of clay minerals

Sr. No.	Clay raw material	Chemical formula	Density (mg/m^3)	Composition (wt%)
1	Kaolin	$Al_2(Si_2O_5)(OH)_4$	2.61	7.17
2	Ball Clay	$3SiO_2.Al_2O_3$	1.80	8.73
3	Feldspar	$(Na, Ca)(AlSi_3O_8)$	3.65	2.78
4	Quartz	SiO_2	2.65	13.21
5	Pyrophallite	$Al_2(Si_2O_5)_2(OH)_2$	2.80	7.31

Steps for preparation of compacts:

- Casting done on gypsum surface or firebricks. Gypsum gives more consistent results
- Compact dried in air for 24 hours at room temperature
- Compacts dried for 24 hours at 100^0C in air
- Further drying at 250^0C for 24 hours
- Sintering at 900^0C for 8-10 hours
- Surface polishing
- Slipcasting
- Second stage sintering

Table 2.2

Optimal conditions for synthesis of zeolite layer

S. No.	Parameter	Values
1.	Hydrothermal crystallization temperature	180^0C
2.	Crystallization time	2-5 days
3.	Pressure attained	150-200 psi
4.	Calcination time	15-20 hrs
5.	Calcination temperature	400^0C

Composition of the synthesis gel

Compound	Weight in grams
Quartz	3.960
Aluminium oxide	1.682
Sodium Hydroxide	4.260
Tetra Propyl ammonium bromide	13.300
Distilled water	100.00

Table 2.3

Specifications of the final membrane

- Effective diameter of the membrane → 6.4 cms
- Effective filtration area → 32.17 cm2
- Membrane thickness → 2-3 mm

Specifications of the Aluminium casing

- OD of the casing → 76 mm
- ID of the casing → 68 mm
- Height of the casing → 5 mm

Table 2.4

Optimal conditions for the synthesis of mesoporous silica

S.No.	Parameter	Values
1.	Hydrothermal crystallization	80^0C
2.	Crystallization time	1-2 hours to 1 week
3.	Pressure attained	80-100 psi
4.	Calcination time	4 hrs
5.	Calcination temperature	500-550^0C

Composition of the synthesis gel for the preparation of mesoporous silica layer

S.No.	Compound	Weight in grams
1.	Hydrochloric acid	15
2.	Tetraethyl ortho silicate	2.314
3.	Cetyl trimethyl ammonium bromide	2.188
4.	Distilled water	100

CHAPTER 3

Results and Discussion

3.1 Development of ceramic compacts

For the synthesis of the clay supports, the various clay ingredients are mixed with water, in the composition given in Table 2.1, to from a thick paste. The paste is cast in shallow aluminium rings and the clay compacts are dried thoroughly in three sequential drying stages given below:

1. Air-drying under ambient conditions for one day
2. Drying in an oven at 100^0C for 24 hrs after air drying
3. Oven drying at 250^0C for 24 hrs after stage 2 drying.

Slow drying of the compacts is a very important step. It is observed that if the drying process is fast and non-uniform, then cracks start developing on the clay surface. Fig 3.1 contains the photographs showing the steady development of cracks with time on a clay compact which is cast on a insulting firebrick or any other surface like glass, steel etc. The reasons for the development of cracks on the clay support surface are given below:

1. It is suggested that fast evaporation of water from the clay compact is responsible for developing stresses in the compact. This results in the development of cracks on the surface, which increase gradually as the drying progresses.

2. When the compacts are placed horizontally during stage 2 and 3 over the brick and dried, only the upper surface of the compact comes in contact with the dry air resulting in non-uniform drying. This uneven drying also gives rise to the development of surface cracks. We eliminated the surface cracks by controlling the drying and by changing the orientation of the compact in stage 2 and 3 to avoid uneven drying. It is observed that by drying the compacts on a Gypsum surface during stage 1, the surface cracks are completely eliminated, whereas by drying the compact on a firebrick surface, the surface cracks are prominent. This might be due to surface properties of firebrick and gypsum. The firebrick surface being

highly porous is likely to give fast driving of the moisture from the clay compact resulting in rapid absorption of water leading to cracks in the compact. On the other hand, the gypsum surface draws the moisture from the compact slowly resulting in slower water removal from the clay compact. Most of the water removed from the compact is available on the gypsum surface as shown in fig 3.2. Taking these precautions, the flat compacts of ceramics were thus prepared. During oven drying at 100^0C and 250^0C, the compacts in the green state are placed vertically over grooves cut on brick surfaces. Due to the vertical orientation, the drying air comes in contact with the compacts from all the sides resulting in uniform drying. Preparation of porous supports using various other materials like refractory castable, geoploymers etc was previously done. But it was observed that these supports lacked strength and were highly porous.

3.2 Sintering Process

After through drying in stage 2, the compacts are sintered in a furnace at 900^0C for 8-10 hrs. Sintering is done to provide the desired strength to the green state clay compacts after stage 1 and stage 2 drying. During sintering, number of structural changes and reactions occur which are given below[66].

1. The clay particles condense together into a crystalline hard and rigid compact that has strength.

2. Between 450-700^0C, the water of crystallization in Kaolin is eliminated producing metakaolin $Al_2Si_2O_6$ as shown in the following reaction

$$Al_2Si_2O_5(OH)_4 \rightarrow Al_2Si_2O_6 + 2H_2O \qquad (3.2)$$

Kaolin metakaolin gas

3. Dehydration of aluminium hydrates occurs in the range 320-560^0C

4. Decomposition of Calcium carbonate giving CO_2 occurs at 830-900^0C

5. Fine organic matter in ball clay is oxidized between 200-700^0C

These gaseous products are expelled during sintering resulting in a volume expansion and formation of pores within the clay compact.

3.3 Warping defects and non uniform surface flatness during sintering

As described above, lots of gaseous products are evolved during sintering and there occurs a volume expansion of the clay compact. This leads to warping leading to non-uniformity in the surface flatness. It is observed that if the clay compacts are not dried beforehand, the warping defects increase due to the extremely rapid removal of water during the high temperature sintering. Also if the compacts are placed horizontally on an insulating brick and kept for sintering, the upper surface is exposed to high sintering temperature leading to uneven sintering and warping defects to a greater extent. The warping defects during the sintering can be reduced by following these precautions.

1. Complete removal of the moisture from the compacts before the sintering.

2. By controlling the heating rate of the furnace, the gaseous products are expelled slowly from the compacts leading to fewer stresses and warping.

3. The compacts should be placed vertically so that most of the surfaces of the compact are subjected to the sintering temperature. This gives less warping and surface defects.

It is observed that even after following all the above precautions, complete elimination of the warping is not possible although it can be reduced to a large extent. The surface non-uniformity in such cases is taken care of by polishing the sintered compacts on a fine silicon carbide abrasive paper (No.-C220). The final geometry of the clay support is a circular macroporous disk with completely flat surface and this allows water to pass through under gravitational forces alone.

3.4 The slipcasting process

In the slipcasting process, the macroporous support as prepared in section 2.1 is coated with a thin mesoporous film by dipping it in a thick kaolin solution, until all the pores of the support get filled with the kaolin sol. This is indicated by the disappearance of the bubbles. After sintering, this kaolin sol inside the pores of the compact condenses into a crystalline, hard material reducing the macroporosity. After thorough washing, the slipcast supports are dried. The weights of the supports are taken before and after the slipcasting process and the typical results are tabulated in Table 3.1a. From the results, it is clearly seen

that a weight gain of the order of 0.1 grams has taken place, which indicated the deposition of a thin mesoporous layer. After slipcasting, the supports are flat and mesoporous with smooth surfaces and this results in higher strength of the supports.

3.5 Deposition of Mesoporous silica in slipcast mesoporous compacts.

Mesoporous silica is fine powder having large pores and surface area of the order of 1200 m^2/g. We have deposited a thin mesoporous layer of silica, having high surface area, over the above slipcast supports by hydrothermal crystallization at 80^0C in an autoclave (parr 1 litre) under autogeneous pressure. The composition of the reaction mixture is as given in Table 2.4. Before and after the reaction, the weights of the supports are recorded as indicated in Table 3.1b. It is clearly seen from the results that after the reaction, the mass of the support decreases. This loss in weight is of the order of 2.5-3 grams, which indicates that in the presence of an acid, the support material is dissolved and this acidic reaction mixture is unsuitable. Moreover, the strength of the supports after this reaction seems to reduce considerably and we then deposited zeolite layer under basic conditions.

3.6 The zeolite deposition reaction

The hydrothermal crystallization of zeolite layer within the mesoporous clay supports under basic medium is done by preparing the aluminosilicate zeolite solution first. This is poured over the slipcast compacts placed at the bottom of an autoclave and reacting the mixture at 180^0C under autogeneous pressure. The composition of aluminosilicate solution and optimal conditions of the reaction are given in Table 2.2. The time of the reaction is altered from 1 day to 5 days, and the corresponding change in the weight of the mesoporous compacts is noted, as shown in Table 3.2 a. It is observed that for all reaction times, gain in weight of the supports occurs indicating the formation of a thin, dense zeolite film on the support. Also it can be seen from the results that the gain in weight of the support reaches an asymptotic value after running the reaction for 3 days (around 3-3.5 g) whereas for 4 day and 5-day reactions, the weight gain is almost constant. In view of this, we chose 3-day reaction time for the deposition of zeolite layer over clay supports. The

deposition of the zeolite layer after 1 and 2 days is negligible as indicated by a very small weight gain. After the reaction is complete, the strength of the support is unaltered and this reaction method, under basic conditions, successfully deposits the zeolite over clay supports without any leaching. In order to burn out the organic surfactant molecules entrapped within the micelles, the zeolite membranes are calcined at 400^0C for 10 hrs. During calcination, the surfactant molecules are burnt leaving behind an open pore zeolite framework. A slight weight loss of the membrane after calcination is shown in Table 3.2 b and it indicates the removal of the organic template ions (TPAB) from the zeolite. It is observed that after the calcination the zeolite films remain stable.

3.7 Structural analysis through Scanning Electron Microscopy (SEM)

In order to study the geometry of the zeolite layer on the clay support, we have carried out the Scanning Electron Microscopy (SEM) of our zeolite membrane. Fig 3.3 shows the SEM photographs of these zeolite layers. These figures reveal that pore openings observed in the SEM photograph of plain substrate have been blocked with a dense, white zeolite film after the reaction. We have also carried out the Scanning Electron Microscopy (SEM) of the zeolite powder crystals that were formed in the autoclave, after the reaction. Figure 3.4 shows the SEM photographs of these zeolite crystals, which reveals that, the structural framework is highly crystalline with uniform geometry.

3.8 XRD of zeolite layer deposited within mesoporous compacts

In order to carry out the structural characterization of this thin zeolite layer, a piece of the compact was broken and its X-Ray Diffraction (XRD) pattern recorded. During all the XRD-analysis, the X-Ray wavelength is kept constant at 1.5406 A^0 and the relative intensity of the diffraction is recorded as the function of 2θ. We have used the XRD data reported in JCPDS file[76] for the structure characterization of our zeolite later deposited. This file has a record of about two hundred zeolites and we compared our XRD result with most of the data. For this, we have first chosen the first five strong XRD peaks of our zeolite layer and reported their relative intensities versus d-values in the Table 3.3. Then we searched the

XRD of the zeolite from the JCPDS file whose first five strong XRD peaks gets matched approximately with the five strong XRD peaks of our zeolite layer. The same table shows the comparative XRD values of the zeolite formed and its most closely matching standard zeolite chosen from JCPDS files. We found that the XRD values of the zeolite, Nepheline Hydrate in file number 10-460, closely matched with the XRD data of our zeolite layer formed. The percentage relative crystallinity of our zeolite compared to its most closely matching standard zeolite, is found by taking ratio of the sum of the relative intensities (all five strong XRD peaks) of the zeolite formed to the sum of the relative intensities (all five strong XRD peaks) of the Nepheline Hydrate zeolite from the JCPDS file. It is found that the percent relative crystallinity of the synthesized zeolite is around 98 %. Various other structural properties of Nepheline Hydrate are also reported in JCPDS file.

3.9 The Bubble Point Technique

For advantages given in Sec. 2.4.3, the Bubble point technique has been chosen for the pore size determination of the membrane. In our case, water is chosen as the wetting liquid and butanol, as the non-wetting liquid due to their large differences in surface tensions[73]. The pressure difference Δp needed to expel butanol from a pore with radius r is given by equation (2.4.3).

An experimental setup shown in Fig 2.1 is used for the measurement of pore size. Initially the zeolite membrane after calcination was placed directly in the base plate over a diaphragm made of cork, above which the cell was assembled. It was observed that the zeolite membrane could not withstand the pressure of the cell and the o-rings leading to frequent cracking of the membrane. To overcome this problem, we developed shallow aluminium metal casing with number of perforations at the bottom, for housing the zeolite membrane. The casing specifications have already been mentioned in Table 2.3. The membrane is housed inside this casing as described in Sec. 2.4.3. Fig 3.2 shows the photographs of the aluminium casing and the final membrane housing arrangement. This casing works and can withstand the pressure of the cell and the o-rings comfortably without

causing any cracking of the membrane. This membrane housing has been successfully used for the ultrafiltration experiments.

3.10 The Flow-Pressure curve and the Pore size of the zeolite membrane

First, the membrane is brought in contact with water as the wetting liquid until all the pores of the membrane get filled with it. This water is held in the pores by capillary forces and it exerts a capillary pressure on the pore surfaces. When external pressure is applied on the membrane, water acts as a barrier and no flow can occur until the pressure difference on the membrane reaches the capillary pressure. After increasing the pressure over this limit, water is expelled from the largest pore first and the other fluid (butanol) then permeates inside. As the pressure of the gas is increased, the remaining smaller pores are opened and butanol permeates into them. At every pressure value, the flow rates of butanol and water and the pressure at which butanol flow just occurs, are recorded for the slipcast support, unmodified zeolite membrane and modified membranes (nitrated and aminated). Tables 3.4-3.5 show these typical results of the membranes by the Bubble point technique. The flow rates of butanol and water are plotted against the applied pressure difference (Δp) and these flow verses pressure drop curves, are usually referred to as the 'S-shaped' flow-pressure curves. Fig.3.8 shows the flow-pressure curves of the slipcast support and the unmodified and modified membranes and from these it is observed that upto a certain Δp, there is no flow and the wetting liquid acts as a barrier. At higher pressures, the flow rate is found to increase and at a certain pressure, it meets the water flow rate curve. It is suggested that at this point, all the pores are available for permeation. By using equation (2.4.3) with the knowledge of surface tensions of both fluids and contact angle values, these pressures have been employed to obtain the pore-size range for the membranes. Table 3.6 contains the final pore size range calculated for the slipcast support, zeolite membrane, nitrated and aminated zeolite membrane. From the tabulated results it can be clearly seen that after the zeolite deposition, the pore size reduces by 75 percent. After nitration and amination, the pore size reduces only by 20 percent and 16 percent respectively as compared to the zeolite membrane. Pore size determination of zeolite membranes with deposition times of 1 to 5 days show that the pore diameters for deposition times of 3 to 5 days is more or less unchanged (see Table 3.6).

3.11 Nitration of the zeolite membranes

Nitration of the zeolite membranes has been carried out by the gas phase nitration reaction at 225^0C as described in the section 2.5. It is observed that for a single run nearly 18 hours of reaction time is needed for the complete consumption of 500 ml of NO_x gas by the zeolite membrane sample. It is found that during the reaction, water is adhered to the wall of the glass reactor. This water is removed from the reactor before it is filled with NO_x to start the next run. After every run we have determined the change in weight of the zeolite membrane and Table 3.7a shows that there is an increase in weight of the membrane. However as the extent of nitration is increased, the strength of the membrane appears to go down and small cracks start developing on the surface. Therefore we have used a maximum of 2000 cc of NO_x divided over four sequential nitration runs. We have presented the photographs of the modified zeolite membranes in Fig 3.9, which shows the change in color of the zeolite membrane from cream (Fig 3.9a) to orange-brown upon nitration (Fig 3.9b). The amination reaction of this nitrated membrane results in a darker color as shown in Fig 3.9c.

3.12 Mechanism of nitration reaction of zeolite membrane

The reactions of NO_x have been extensively studied in literature of the area of pollution[74, 75]. The reaction is assumed to be triggered by nitrogen and NO_2 and in their presence oxygen radical (O^0) is formed as follows

$$NO_2 \rightleftharpoons NO + O^{\bullet} \qquad (3.12a)$$

This oxygen radical reacts with moisture to give hydroxyl radicals as follows

$$H_2O + O^{\bullet} \overset{NO_x}{\rightleftharpoons} 2OH^{\bullet} \qquad (3.12b)$$

$$H_2O \overset{NO_x}{\rightleftharpoons} OH^{\bullet} + H^{\bullet} \qquad (3.12c)$$

These hydroxyl and hydrogen radicals are active species, which are assumed to give reactions involving NO_X. The zeolite layer, which has been deposited, consists of Si and Al tetrahedron connected by common oxygen sharing (species a). During the gas phase

nitration, the Si-O bond is broken in the presence of NO_x (giving species b and c) as follows.

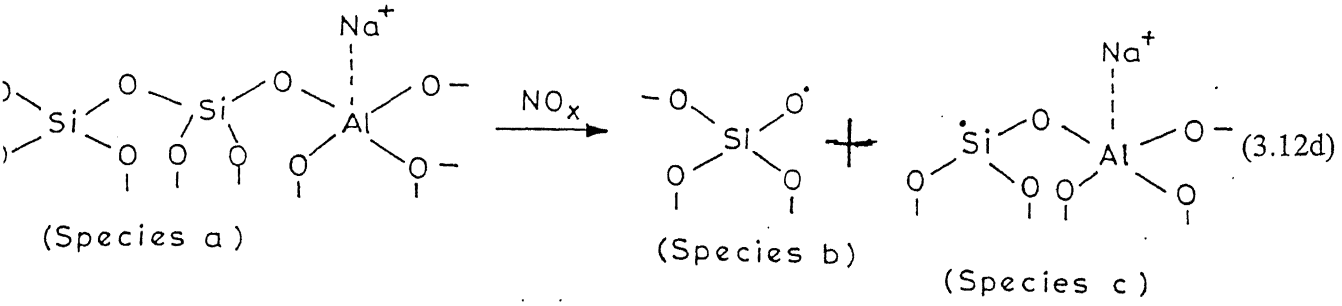

(3.12d)

This oxygen radical of species b reacts with hydrogen radical (H^0) to give the hydroxyl functional group (species d) as shown below.

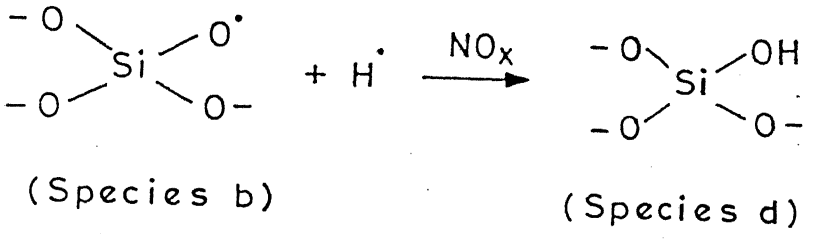

(3.12e)

The active H^0 radical again reacts with the hydroxyl group, which creates an active site on the silicon (Si) atom (species e) as shown below

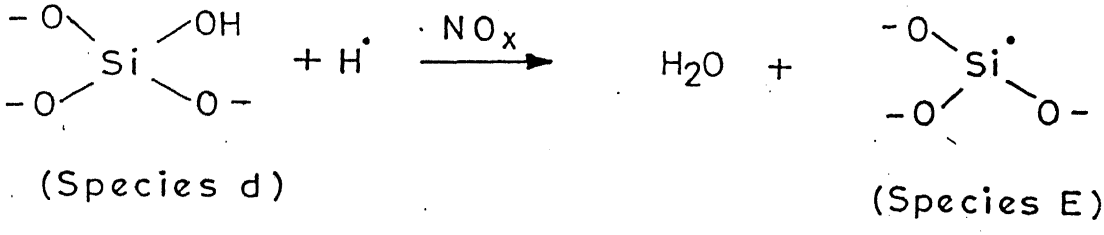

(3.12f)

In addition to this, the water of hydration is also released which is found to adhere to the wall of the glass reactor. The active site on the silicon (Si) atom of the zeolite layer as well as the support, now easily reacts with NO_2 (which is a stable radical) present in NO_x to give $-NO_2$ group attached to the Si atom as follows.

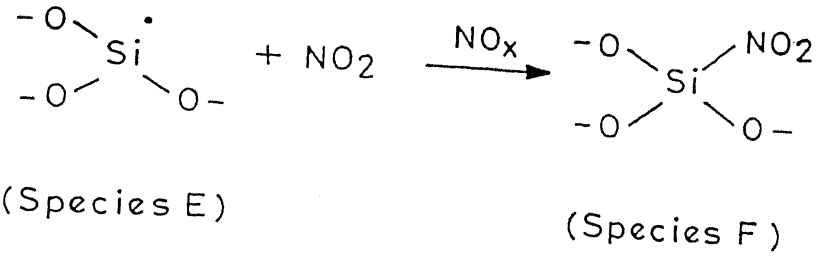

(3.12g)

3.13 Amination of zeolite membrane

Amination of the zeolite membrane is carried out in the presence of 50 % Hydrazine Hydrate. The $-NO_2$ group of nitrated zeolite is converted into an $-NH_2$ amine group by amination. The concentration of Hydrazine Hydrate is critical as it is observed that its large concentration affects the strength of the material adversely and a leaching of the support material occurs. At around 50 % Hydrazine Hydrate, the porous support as well as the zeolite layer are stable and a considerable increase in weight of typical samples is shown in Table 3.7b.

3.14 Anion exchange capacity of Modified membrane

The anion exchange capacity of the aminated membrane is due to the amine group ($NH_3^+Cl^-$) and is determined by the standard procedure discussed in the section 2.7. The Table 3.8 gives the anion exchange capacity of the aminated membranes in meq per gram of the oven dry mass of the membrane. It is found that the average value of anion exchangeability of our modified zeolite membrane is 0.8 meq/g and it increases with the increase in the silica content of the zeolite. This is because the Si atom of the zeolite gives the Si-N bond.

3.15 Crystallographic study of Modified Zeolite membrane

We have recorded the XRD pattern of the nitrated zeolite membrane in order to study the crystallographic changes in it due to nitration. In figures 3.5-3.7, we have

presented the XRD patterns of unmodified and modified zeolite membranes. It is observed that the XRD patterns are altered upon nitration. From the JCPDS cards, we chose the most closely matching standard aluminosilicate zeolite (File No. 25-779) adopting the same procedure discussed earlier in the section 3.8. The Table 3.3 gives the d-spacing and relative intensity values of XRD analysis for the unmodified, nitrated and aminated zeolite membrane and their most closely matching standard zeolite. The molecular structure of this nitrated zeolite layer is $Na_2Al_2Si_2O_7.(OH)_2$. The presence of the hydroxyl group on the repeat unit supports the postulated mechanism. This nitrated zeolite layer is found to have 82 percent crystallinity (with respect to standard zeolite, JCPDS File No. 25-779) and has a tetragonal crystal structure. This change in the crystal structure of the zeolite upon nitration confirms that, Si-O bond must have broken. After amination, it is found that there is no further change in the crystal structure but the percent relative crystallinity increases to 84 percent.

3.15 Ultrafiltration experiments using a surfactant

Ceramic membranes have been used extensively in separation and ultrafiltration experiments and some of the more recent applications reported in literature, are summarized in Table 3.9. A careful review of the existing literature indicates that very little work is reported on the effect of chemical modification on the ultrafiltration of solutions. In view of this, our work has focused on the study of effect of modification on the rejection and flux in ultrafiltration of a surfactant solution using zeolite membranes. This ultrafiltration can be easily extended to the removal of organic impurities by trapping them within the surfactant miscelles, referred to as micellar-enhanced ultrafiltration.

A cationic surfactant Cetyl Pyridinium chloride (CPC) has been used in our ultrafiltration experiments. A 2-weight percent surfactant solution (around 600 ml) is used in the experiment for a single membrane sample. The ultrafiltration is carried out by the method described in section 2.9. The permeate and the retentate concentrations, at different pressures, are determined from conductivity calibration curve show in Fig 3.10, which is calibrated using standard CPC solutions and 0.1 N KCl. The percent rejection of the surfactant solution is calculated using the equations of Sec. 2.8. The steady state surfactant

flow rates are determined experimentally at different pressures. The plot of percent rejection versus applied pressure has been plotted for the unmodified, nitrated and aminated membranes in Fig. 3.11. From this figure, it can be observed that as the applied pressure increases the percent rejection gradually decreases. For all the three cases, an objective function has been defined which is a product of the separation achieved by the membrane and the surfactant flow rate given by

$$OF = \frac{\text{surfactant}}{\text{flow rate}} \times \left(\begin{matrix} \text{wt\% in} \\ \text{retentate} \end{matrix} - \begin{matrix} \text{wt\% in} \\ \text{permeate} \end{matrix} \right) \qquad (3.15)$$

These objective function values have been calculated and plotted against the pressure for the unmodified and modified membranes. The plot is shown in Fig 3.12. It has been observed that the OF curves reach a maximum which corresponds to the optimum rejection pressure. From this figure, it can be seen that the optimum pressures for rejection, in all the three cases, is in the range of 40-44 psi. All the ultrafiltration results for the unmodified nitrated and aminated membranes are summarized in Table 3.10-3.12 and it is clearly seen that there is a considerable increase in rejection due to modifications. These rejection values are 28% for unmodified membrane, 58% for nitrated membrane and 76% for aminated membrane, at the optimum pressure condition. Thus modification of the zeolite membrane has considerably improved the rejection. Another important result that can be noted from these tables is that with modification, the ratio of surfactant to water flow rate is found to increase. The ratio is 0.3-0.4 in unmodified membrane, around 0.6 in nitrated and 0.7-0.8 in aminated membrane. These values could be compared to the literature value in which this ratio was reported to lie in the range of 0.09-0.1 for commercially available ceramic membranes with pore size of 200 A^0 (rejection of 60%). This increase in the ratio with modification clearly indicates the increase in the affinity of the modified membranes for water i.e. the increase in the hydrophilicity.

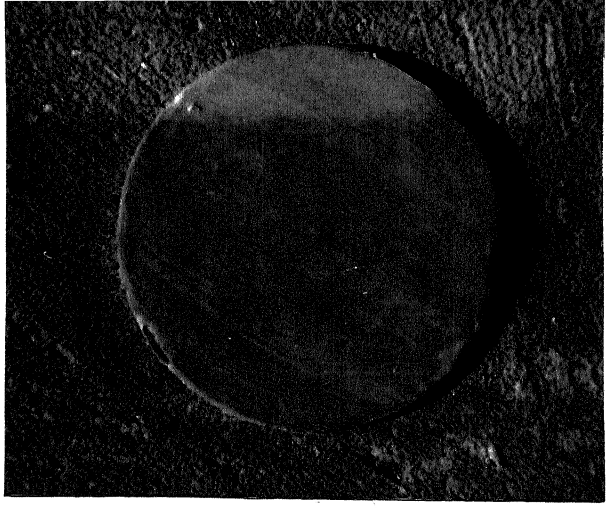

(a)

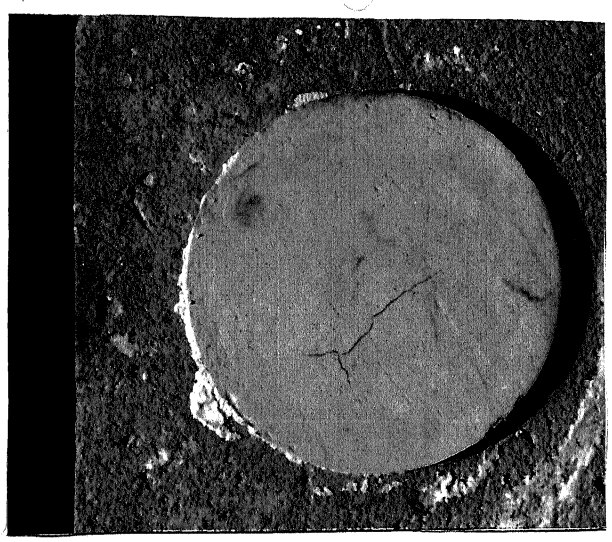

(b)

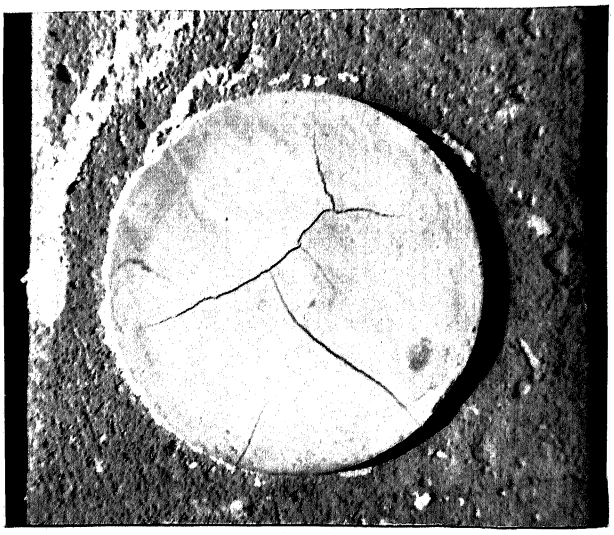

(c)

Figure 3.1: Steady development of cracks on the clay compact placed on the brick surface, with time (a) wet support (b) after 4 hrs and (c) after 12 hrs

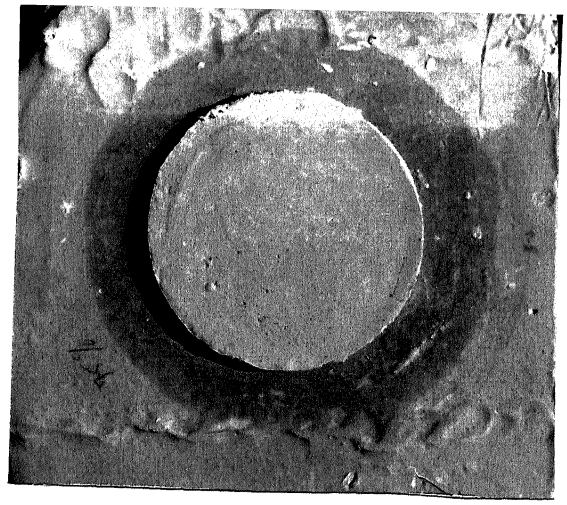

(a)

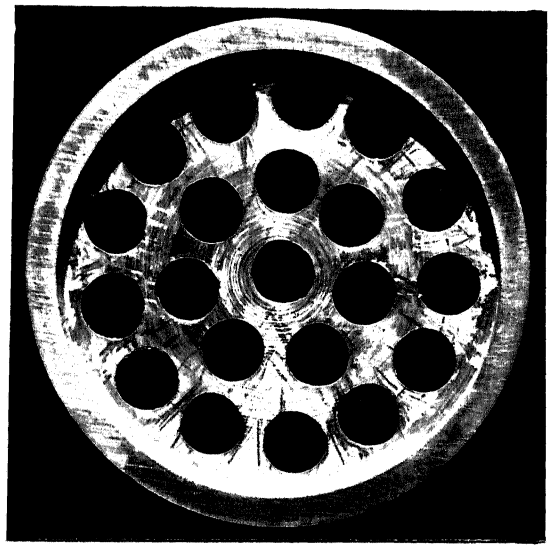

(b)

(c)

Figure 3.2: Photographs of (a) gypsum surface holding water (b) Aluminium casing and (c) final membrane housing arrangement

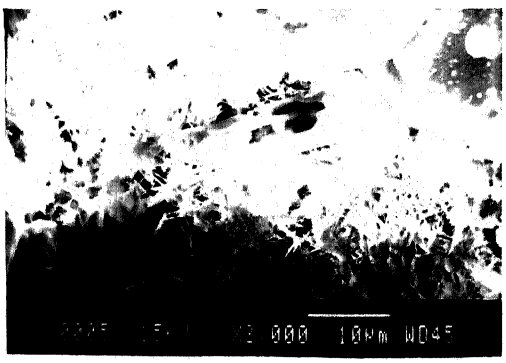

Figure 3.3: SEM photograph of zeolite layer deposited on mesoporous clay supports

Figure 3.4: SEM photograph of zeolite powder crystals formed in the autoclave during hydrothermal synthesis

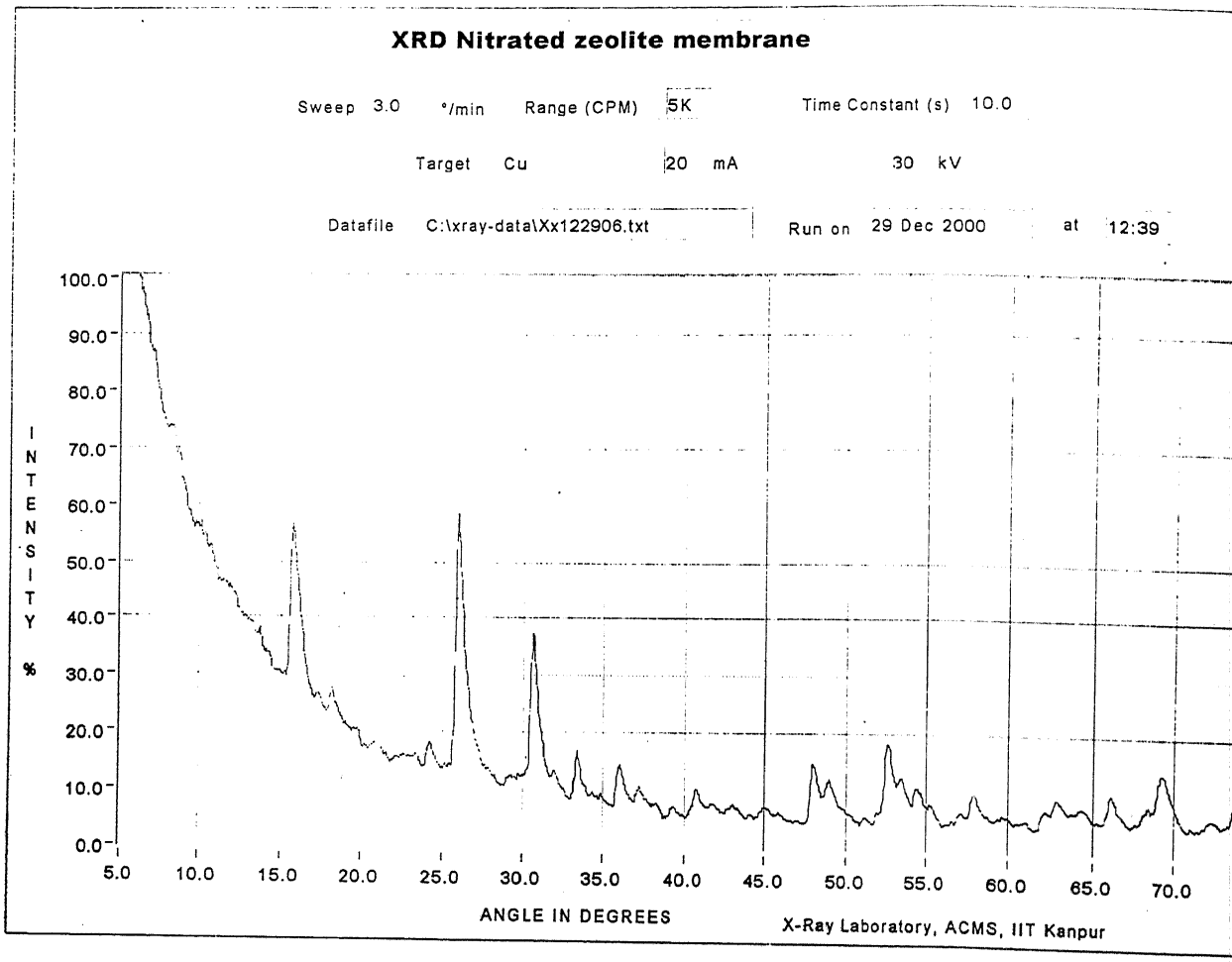

Figure 3.6: XRD pattern of Nitrated zeolite membrane

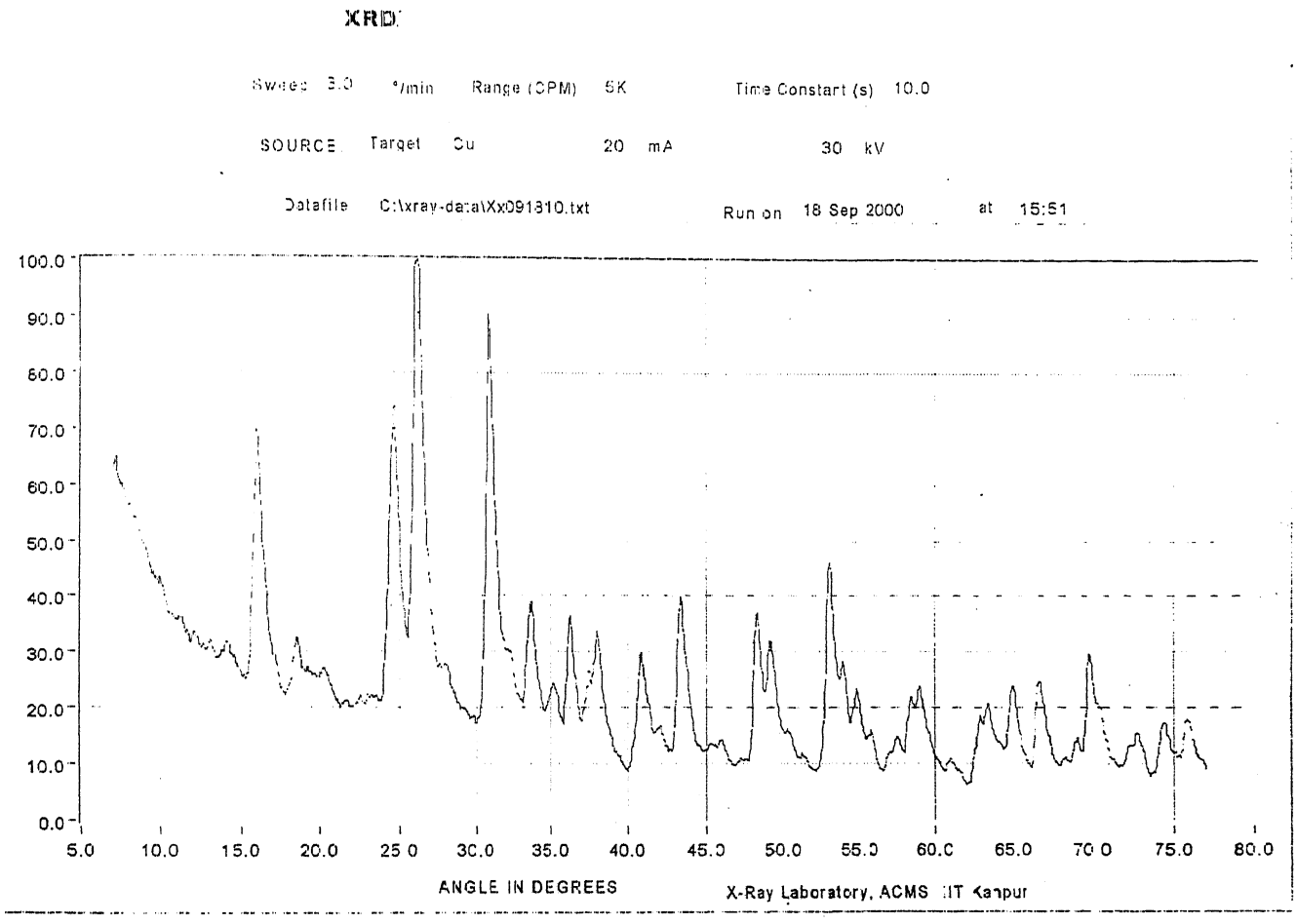

Figure 3.5: XRD pattern of unmodified zeolite membrane

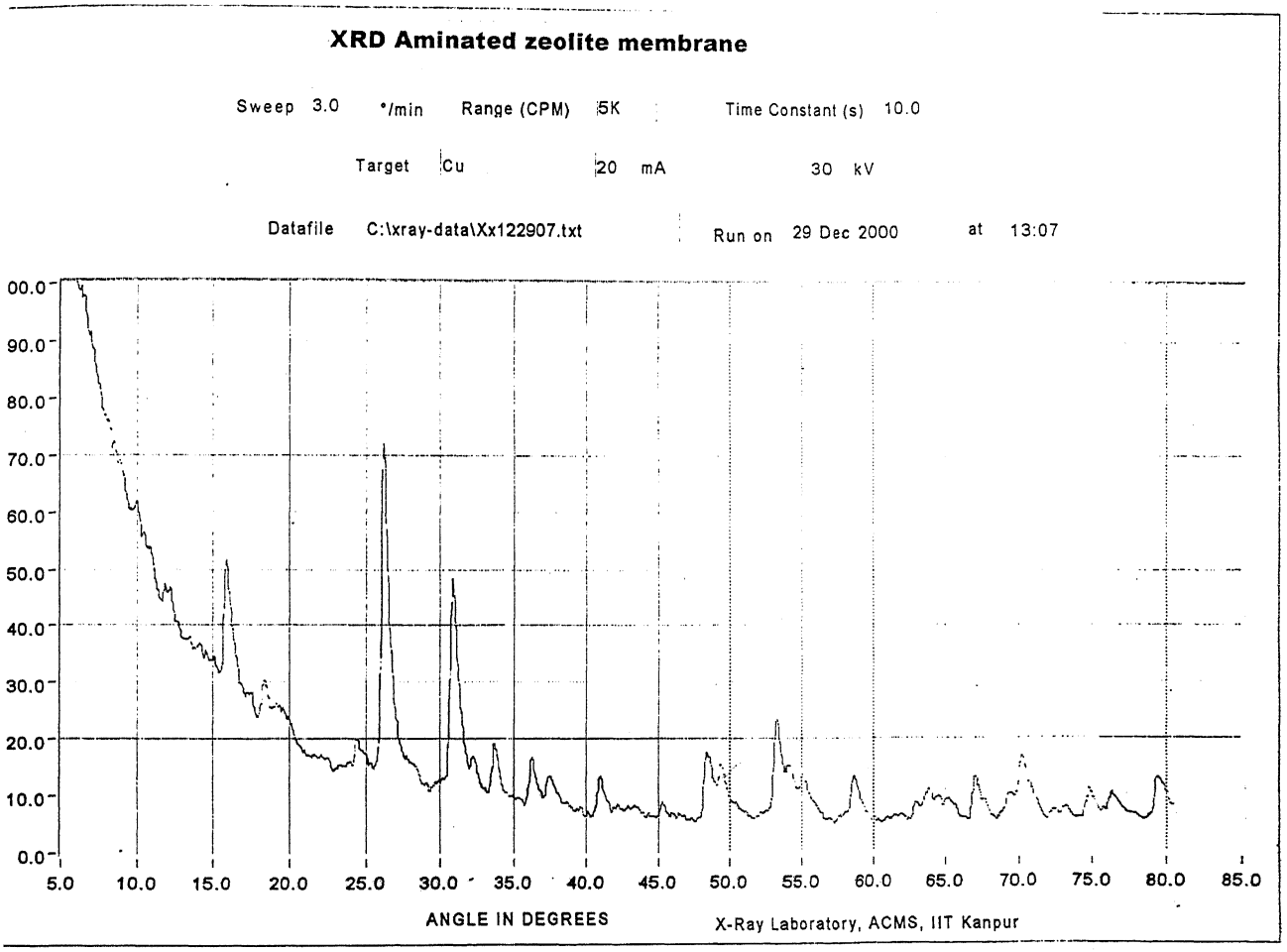

Figure 3.7: XRD pattern of Aminated zeolite membrane

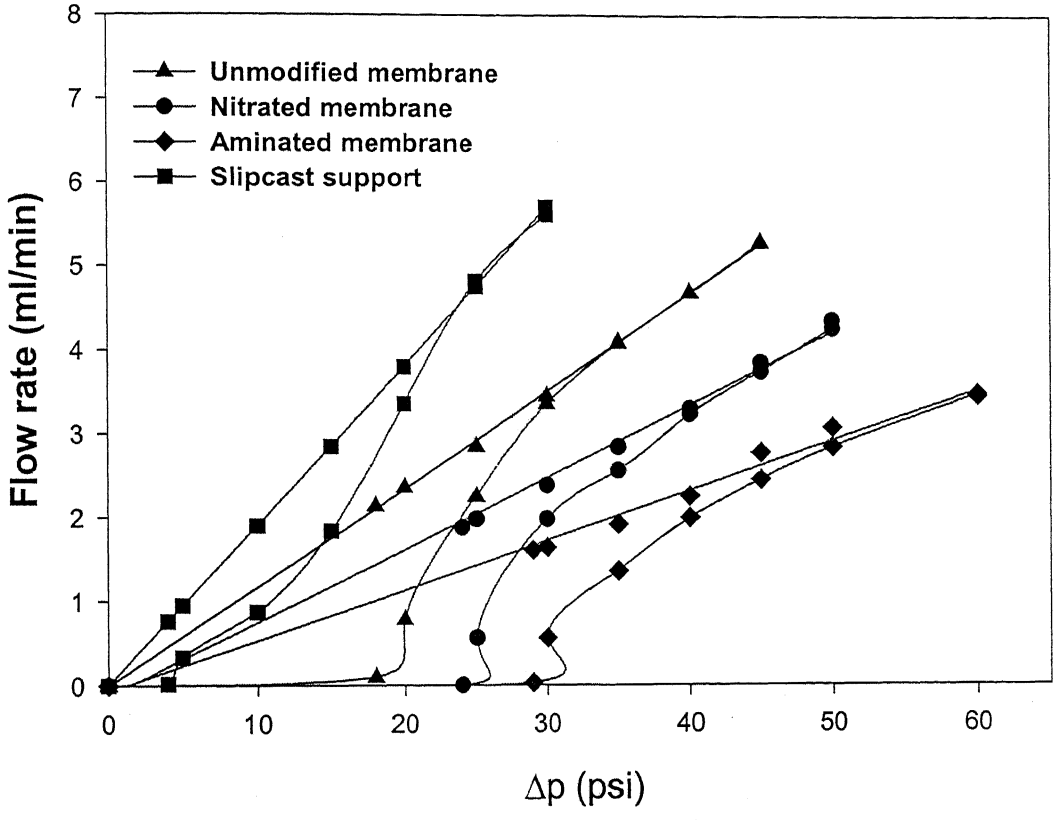

Fig 3.8: Flow pressure curves of slipcast support, zeolite membrane, nitrated and aminated zeolite membranes

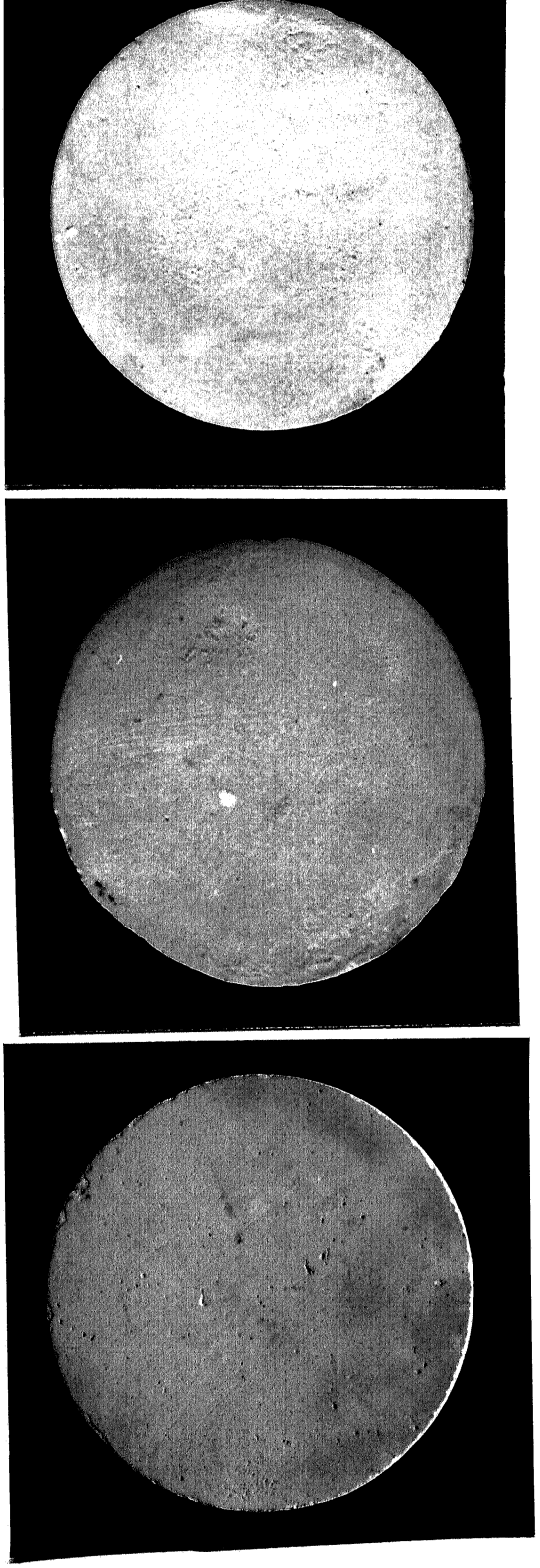

(a)

(b)

(c)

Fig. 3.9: Photographs of (a) unmodified (b) nitrated and (c) aminated zeolite membranes

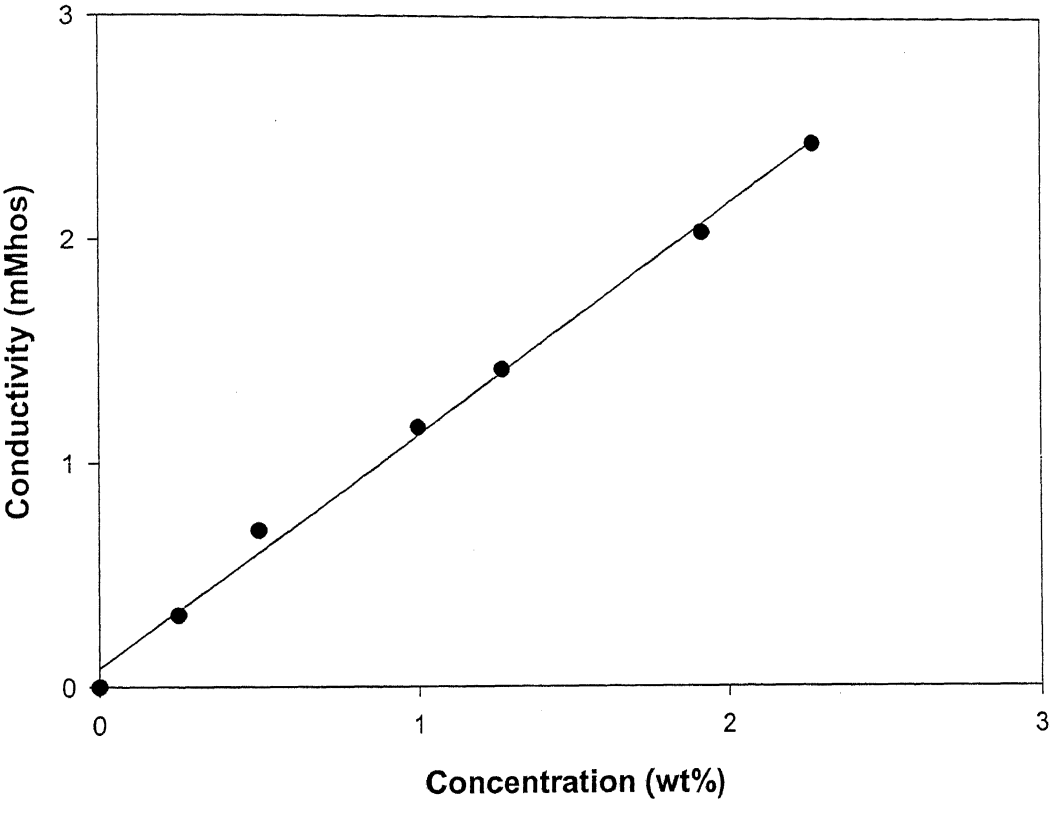

Fig 3.10: Calibration curve for Cetyl pyridinium chloride (CPC) concentration

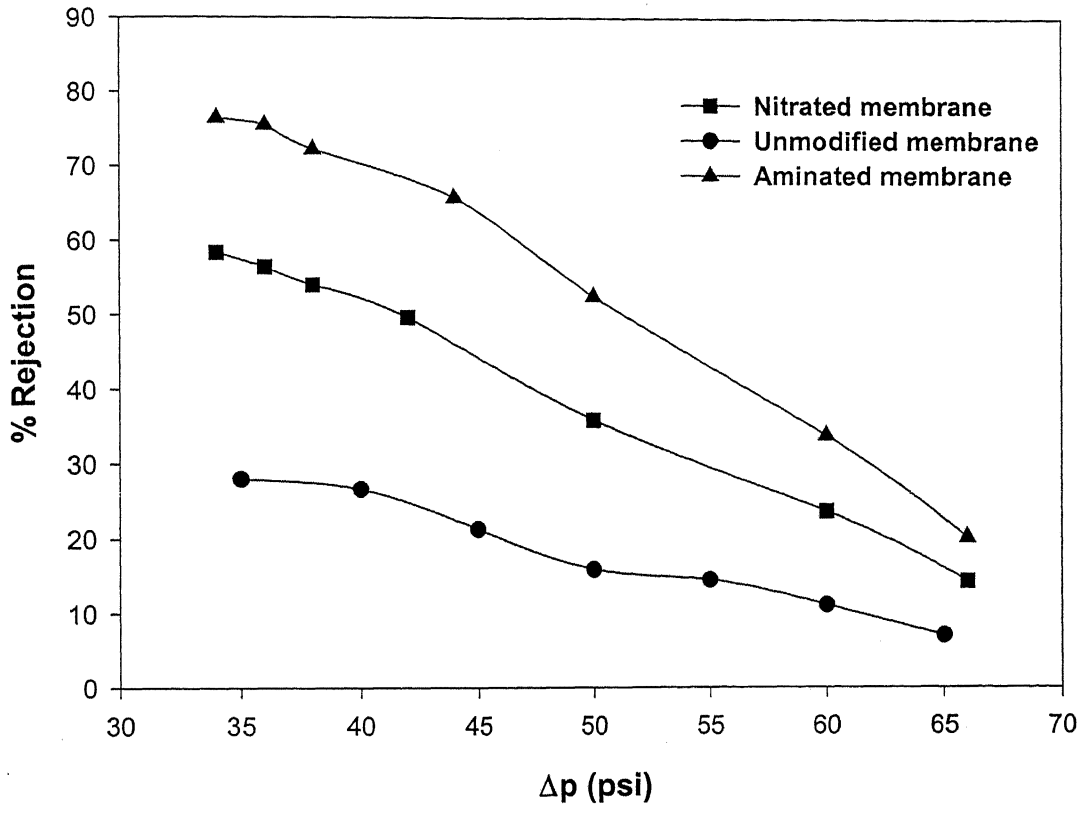

Fig 3.11: Rejection curves for unmodified and modified zeolite membranes.

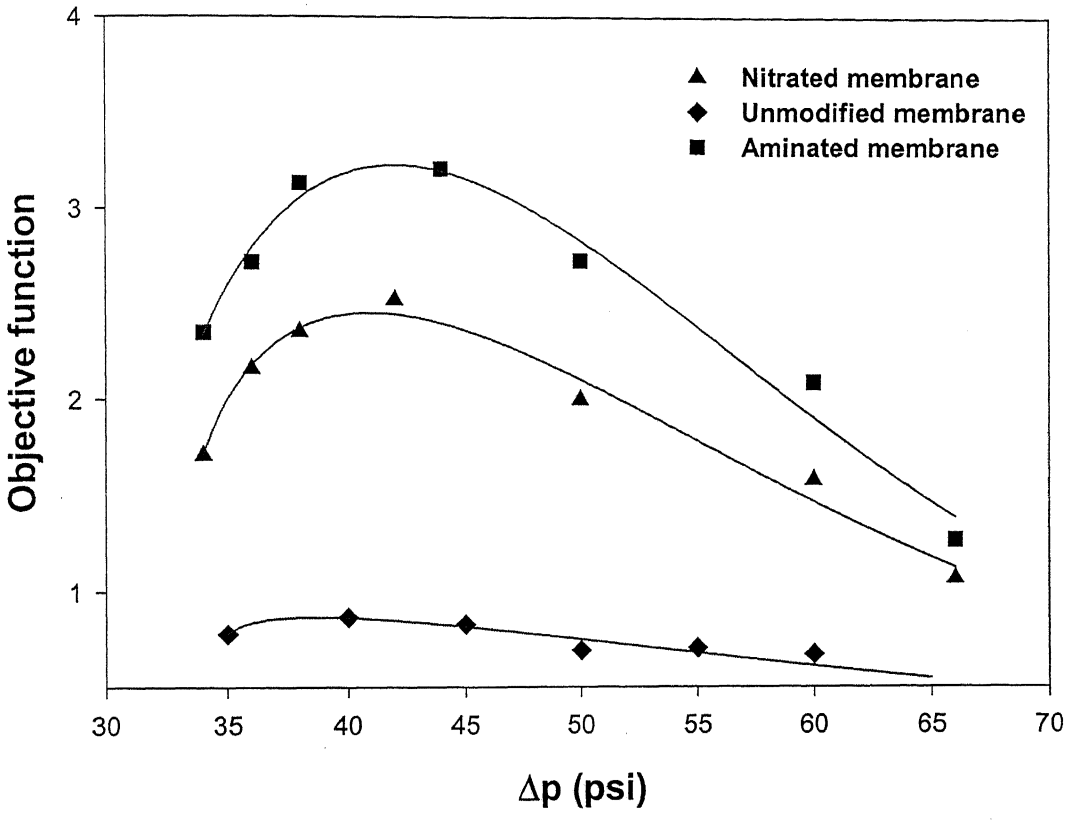

Fig 3.12: OF (defined in eqn. 3.15) versus applied pressure for rejection in ulrafiltration

Table 3.1
Changes in weight of macroporous ceramic support after further processing

(a) Change in weight due to slipcasting

Sr. No.	Sample No.	Weight before slipcasting (g.)	Weight after slipcasting (g.)	Gain in weight (g.)
1	A_1	15.5977	15.6825	0.0848
2	A_2	16.8637	16.9436	0.0799
3	A_3	16.3147	16.3965	0.0818
4	A_4	16.4418	16.5332	0.0914
5	A_5	17.7422	17.8209	0.0787
6	A_6	16.2435	16.3110	0.0675
7	A_7	18.1021	18.1988	0.0967
8	A_8	17.2343	17.3102	0.0759

(b) Loss in weight after deposition of mesoporous silica in acidic medium.

Sr. No.	Sample No.	Weight before mesoporous silica deposition (g.)	Weight after mesoporous silica deposition (g.)	Loss in weight (g.)
1	B_1	16.8419	13.9764	2.8655
2	B_2	18.3178	15.1964	3.1214
3	B_3	17.5450	14.5689	2.9761
4	B_4	16.3145	13.0706	3.2439

Table 3.2
Changes in weight of mesoporous ceramic supports after processing

(a) Gain in weight after deposition of zeolite with time of reaction

Sr. No.	Sample No.	Weight before zeolite deposition. (g.)	Reaction time (h.)	Weight after reaction (g.)	Gain in weight (g.)
1	C_1	15.9041	24	17.0418	1.1377
2	C_2	17.4469	48	19.6830	2.2361
3	C_3	16.0200	72	19.3777	3.3577
4	C_4	16.8419	96	20.2421	3.3002
5	C_5	17.0029	120	20.3787	3.3258

(b) Loss in weight after calcination for 72 hours of reaction of samples A_1 to A_8 of Table 3.1a

Sr. No.	Sample No.	Weight after zeolite reaction (72 hrs) and before calcination (g.)	Weight after calcination (g.)	Loss in weight (g.)
1	A_1	18.8059	18.6167	0.1892
2	A_2	20.6647	20.4336	0.2311
3	A_3	19.9867	19.7883	0.1984
4	A_4	19.5209	19.3093	0.2116
5	A_5	21.6348	21.4449	0.1899
6	A_6	19.4200	19.1955	0.2245
7	A_7	21.8659	21.6486	0.2173
8	A_8	20.3116	20.0815	0.2301

Table 3.3
The XRD analysis and crystal structure of modified zeolite on mesoporous support

(a) Comparative XRD values of the zeolite deposited and its most closely matching aluminosilicate zeolite chosen from JCPDS cards

Zeolite/ JCPDS file No.	d_1 value (%RI)	d_2 value (%RI)	d_3 value (%RI)	d_4 value (%RI)	d_5 value (%RI)	ΣRI	Percent crystallinity
Zeolite deposited	3.405 (100)	2.897 (90.64)	3.611 (74.06)	5.523 (68.71)	2.085 (40.03)	373.44	98.27
File No. 10- 460	3.414 (100)	2.950 (90.00)	3.712 (80.00)	5.210 (70.00)	2.195 (40.00)	380.00	
Nitrated zeolite layer	3.424 (56.27)	5.621 (55.99)	2.993 (36.70)	1.737 (18.18)	1.897 (14.71)	181.85	82.65
File No. 25-779	3.320 (60.00)	5.770 (70.00)	2.964 (40.00)	1.735 (30.00)	1.866 (20.00)	220.00	
Aminated zeolite layer	3.406 (71.48)	5.599 (50.80)	2.898 (47.27)	1.719 (23.41)	1.879 (17.37)	210.33	84.13
File No. 31-1271	3.568 (90.00)	5.713 (50.00)	2.976 (60.00)	1.764 (30.00)	1.891 (20.00)	250.00	

(b) Structural characterization of zeolite deposited and standard zeolites using XRD analysis.

Sr. No.	Type of zeolite layer	Molecular structure of aluminosilicate zeolites	Geometry of crystal structure	Molecular weight	Percent relative crystallinity.
1	Unmodified	$Na_2Al_2Si_2O_8.H_2O$	Orthorhombic	302	98.27
2	Nitrated	$Na_2Al_2Si_2O_7.(OH)_3$	Tetragonal	319	82.65
3	Aminated	$(NaAlSiO_2)_x.\ yH_2O$	Tetragonal	-	84.13

Table 3.4
Bubble point data of different unmodified mesoporous supports

(a) Bubble point data for slipcast support

Sr. No.	Pressure (psi)	Butanol flow rate (ml/min)	Water flow rate (ml/min)
1	0	0.00	0.00
2	4	0.02	0.76
3	5	0.33	0.95
4	10	0.87	1.90
5	15	1.84	2.85
6	20	3.36	3.80
7	25	4.82	4.75
8	30	5.61	5.70

(b) Bubble point data for unmodified zeolite membrane.

Sr. No.	Pressure (psi)	Butanol flow rate (ml/min)	Water flow rate (ml/min)
1	0	0.00	0.00
2	18	0.10	2.14
3	20	0.78	2.36
4	25	2.25	2.85
5	30	3.36	3.45
6	35	4.08	4.09
7	40	4.68	4.68
8	45	5.28	5.29

Table 3.5
Bubble point data of Modified mesoporous supports

(a) Bubble point data for nitrated membrane

Sr. No.	Pressure (psi)	Butanol flow rate (ml/min)	Water flow rate (ml/min)
1	0	0.00	0.00
2	24	0.00	1.88
3	25	0.56	1.98
4	30	1.98	2.38
5	35	2.56	2.84
6	40	3.24	3.30
7	45	3.75	3.85
8	50	4.26	4.35

(b) Bubble point data for aminated membrane

Sr. No.	Pressure (psi)	Butanol flow rate (ml/min)	Water flow rate (ml/min)
1	0	0.00	0.00
2	29	0.03	1.61
3	30	0.56	1.64
4	35	1.36	1.92
5	40	2.00	2.26
6	45	2.46	2.78
7	50	2.85	3.08
8	60	3.48	3.46

Table 3.6
Effect of modification on the Pore diameter range of zeolite membranes

(a) Pore diameter ranges after reaction time of 72 hours

Sr. No.	Type of sample	Δp initial (psi)	Δp final (psi)	Pore radius calculated using equation 2.4.3. (A°)		Final Pore diameter range (A°)
				For Δp initial	For Δp final	
1.	Mesoporous slipcast support	5	20	545.5	136	1091-272
2	Unmodified zeolite membrane	20	35	136.5	78.0	273-156
3	Nitrated zeolite membrane	25	45	109	60.5	218-121
4	Aminated zeolite membrane	30	50	90.5	54.5	181-109

(b) Effect of reaction times on pore diameter ranges of zeolite membranes

Sr. No.	Sample No.	Duration of the zeolite deposition reaction (h.)	Pore diameter range (A°)
1	C_1	24	893-297
2	C_2	48	513-212
3	C_3	72	269-152
4	C_4	96	257-159
5	C_5	120	252-162

Table 3.7
Gain in weight of zeolite membranes after modification

(a) Gain in weight after nitration reaction

Sr. No	Sample No.	Weight before nitration reaction (g.)	Weight after nitration reaction (4 runs) (g.)	Gain in weight (g.)
1	A_1	18.6167	19.1489	0.5322
2	A_2	20.4336	21.1307	0.6971
3	A_3	19.7883	20.2873	0.4990
4	A_4	19.3093	19.7084	0.3991
5	A_5	21.4449	21.9950	0.5501
6	A_6	19.1955	19.6728	0.4773
7	A_7	21.6486	22.2603	0.6117
8	A_8	20.0815	20.5974	0.5132

(b) Gain in weight after amination reaction

Sr. No.	Sample No.	Weight before amination reaction (g.)	Weight after amination reaction (g.)	Gain in weight (g.)
1	A_1	19.1489	19.4706	0.3217
2	A_2	21.1307	21.4299	0.2992
3	A_3	20.2873	20.5415	0.2542
4	A_4	19.7084	19.9861	0.2777
5	A_5	21.9950	22.3293	0.3343
6	A_6	19.6728	19.9847	0.3119
7	A_7	22.2603	22.5202	0.2599
8	A_8	20.5974	20.8864	0.2917

Table 3.8

(a) Effect of varying the Si/Al ratio in the reaction mixture on the exchange capacity of modified zeolite membranes.

Sr. No.	Sample No.	Si/Al ratio in the reaction mixture	Mass of the dry membrane (g.)	Mass of AgCl ppt. (g.)	Exchange capacity (meq/g)
1	A_1	1.58	19.4706	2.3342	0.835
2	A_2	2.00	21.4299	2.6564	0.863
3	A_3	2.55	20.5415	2.6113	0.885
4	A_4	3.00	19.9861	2.5823	0.900

(b) Changes made in the various samples during the synthesis of the zeolite membranes

Sr. No.	Sample No.	Changes made during the synthesis.			
		Si/Al ratio	Reaction time (days)	Support thickness (mm)	Slipcasting
1	A_1	1.58	3	4	Yes
2	A_2	2.00	3	4	Yes
3	A_3	2.55	3	4	Yes
4	A_4	3.00	3	4	Yes
5	A_5	2.00	2	4	Yes
6	A_6	2.00	3	2	Yes
7	A_7	2.00	4	4	Yes
8	A_8	2.00	3	4	No

Table 3.9
Ultrafiltration and separation experiments reported in literature using ceramic membranes.

Sr. No.	Ceramic membranes used	Ultrafiltration/separation experiments.
1.	Commercially available α-alumina tubular membrane	Ultrafiltration involving separation of solute (benzene) from cationic and anionic surfactants[7].
2.	Composite microporous glass membrane on ceramic tubing	Separation of gaseous mixtures of CO_2 and CH_4[13]
3.	NaY zeolite membrane	Pervaporation experiments of Methanol-methyl tertbutyl ether mixtures[26].
4.	A tubular commercial γ-alumina membrane	Separation of CH_3OH/H_2 and CH_3OH/CH_4 mixtures[44].
5.	Silicalite layer grown on commercial ceramic disks	Gas permeation experiments involving He/N_2, n-butane/N_2, and n-butane/i-butane[47].
6.	ZrO_2 deposited on porous carbon tube, modified by a polymer coating	Extraction of α-lactalbumin from whey protein concentrate[64].
7.	Zircon layer coated on a porous carbon tube	Ultrafiltration of Cetylpyridinium chloride solutions[77].
8.	Commercial porous alumina disk	Ultrafiltration of soyabean oil/hexane extract[78].
9.	γ-alumina porous disk modified by $CaCO_3$ via deposition	Separation of acetone/water vapor mixtures[79].

Table 3.10
Ultrafiltration results for unmodified A_3 zeolite membrane using 2-wt% CPC.

Sr. No.	Pressure (psi)	Permeate		Retentate		% rejection from equation 2.8c
		Conductivity (mMhos)	Concentration (wt%) from calibration curve	Conductivity (mMhos)	Concentration (wt%) from calibration curve.	
1	65	1.49	1.872	1.59	2.014	7.025
2	60	1.44	1.801	1.60	2.028	11.162
3	55	1.40	1.745	1.61	2.042	14.549
4	50	1.38	1.716	1.61	2.042	15.935
5	45	1.31	1.617	1.62	2.056	21.330
6	40	1.24	1.518	1.63	2.070	26.651
7	35	1.22	1.490	1.63	2.070	28.018

Sr. No.	Pressure (psi)	Surfactant flow rate (ml/min)	Water flow rate (ml/min)	Surfactant/Water ratio	Objective function from equation 3.15	Membrane resistance (R_m) Water rate/ press
1	65	3.520	7.670	0.4589	0.4981	-
2	60	2.960	7.112	0.4161	0.6701	0.1116
3	55	2.370	6.510	0.3640	0.7042	0.1204
4	50	2.125	5.870	0.3620	0.6916	0.1280
5	45	1.889	5.290	0.3571	0.8288	0.1160
6	40	1.570	4.688	0.3348	0.8664	0.1204
7	35	1.340	4.090	0.3276	0.7774	0.1196

Table 3.11
Ultrafiltration results for nitrated A_3 zeolite membrane using 2-wt% CPC.

Sr. No.	Pressure (psi)	Permeate		Retentate		% Rejection from equation 2.8c
		Conductivity (mMhos)	Concentration (wt%) from calibration curve	Conductivity (mMhos)	Concentration (wt%) from calibration curve	
1	66	1.82	1.692	2.1	1.976	14.348
2	60	1.72	1.585	2.2	2.082	23.774
3	50	1.48	1.333	2.2	2.082	35.958
4	42	1.26	1.100	2.3	2.187	49.682
5	38	1.17	1.005	2.3	2.187	54.030
6	36	1.12	0.952	2.3	2.187	56.446
7	34	1.08	0.910	2.3	2.187	58.379

Sr. No.	Pressure (psi)	Surfactant Flow rate (ml/min)	Water flow rate (ml/min)	Surfactant/Water ratio	Objective function from equation 3.15	Membrane resistance (R_m) Water rate/ press
1	66	3.78	5.600	0.6750	1.0719	-
2	60	3.20	5.150	0.6213	1.5840	0.0750
3	50	2.67	4.140	0.6449	1.9990	0.1010
4	42	2.32	3.487	0.6652	2.5217	0.0815
5	38	1.99	3.120	0.6377	2.3524	0.0918
6	36	1.75	2.870	0.6097	2.1611	0.1252
7	34	1.34	2.753	0.4867	1.7115	0.0584

Table 3.12
Ultrafiltration results for A_3 Aminated zeolite membrane using 2-wt% CPC.

Sr. No.	Pressure (psi)	Permeate		Retentate		% rejection from equation 2.8c
		Conductivity (mMhos)	Concentration (wt%) from calibration curve	Conductivity (mMhos)	Concentration (wt%) from calibration curve	
1	66	1.71	1.576	2.1	1.976	20.232
2	60	1.52	1.375	2.2	2.082	33.927
3	50	1.20	1.037	2.3	2.187	52.581
4	44	0.96	0.783	2.4	2.293	65.828
5	38	0.82	0.635	2.4	2.293	72.280
6	36	0.75	0.561	2.4	2.293	75.507
7	34	0.73	0.540	2.4	2.293	76.428

Sr. No.	Pressure (psi)	Surfactant flow rate (ml/min)	Water flow rate (ml/min)	Surfactant/Water ratio	Objective function from equation 3.15	Membrane resistance (R_m) Water rate/ press
1	66	3.180	3.650	0.8712	1.2715	-
2	60	2.960	3.460	0.8554	2.0910	0.0260
3	50	2.370	3.200	0.7406	2.7264	0.0700
4	44	2.125	2.780	0.7643	3.2083	0.1020
5	38	1.889	2.168	0.8715	3.1324	0.1460
6	36	1.570	1.876	0.8368	2.7189	0.0655
7	34	1.340	1.745	0.7679	2.3489	0.0513

Chapter 4

Conclusion

We have synthesized the ceramic-zeolite composite membrane by growing a zeolite layer above a mesoporous ceramic clay support through hydrothermal crystallization. In this thesis, we have found following.

1. The XRD data of the zeolite membranes has been determined using the JCPDS cards. It has orthorhombic crystal structure (98% crystalline) having the formula, $Na_2Al_2Si_2O_8.H_2O$ of Nepheline Hydrate.
2. The pore sizes of these unmodified membranes have been determined using the Bubble point technique and are in the range of 273-156A^0. After modification, a small decrease in the pore size occurs from 273-156 A^0 to 181-109 A^0 without any pore blocking.
3. In order to alter the hydrophilicity of the zeolite membrane, the chemical modification of these has been done using NO_X gas at 225^{0}C. In this reaction, the $-NO_2$ group, bound to the Si atom has been further reduced to an amine ($-NH_2$) group by reaction with hydrazine hydrate.
4. The XRD studies of the nitrated and aminated zeolite membranes have also been carried out which show that the crystal structure of the zeolite deposited changes from orthorhombic (98.27 percent crystalline, formula $Na_2Al_2Si_2O_8.H_2O$) for the unmodified zeolite to tetragonal (82 percent crystalline, formula $Na_2Al_2Si_2O_7.(OH)_3$) for the modified zeolite. This change in the geometry of the crystal structure has been attributed to the breaking of the Si-O-Si bond during nitration.
5. The anion exchange capacity of this modified zeolite membrane has been determined to be around 0.8 meq/dry g. It is found that by increasing the Si/Al ratio in the reaction mixture, the exchange capacity increases. This is because only the Si atom forms a bond with NO_2 whereas the Al does not react with NO_X.
6. These unmodified and modified membranes have been subjected to the ultrafiltration experiments using a surfactant. It has been observed that the rejection capacity of the membranes increases from 28 percent for the unmodified membrane to 76 percent

for the aminated modified membrane. This three-fold increase in the rejection clearly indicates the improvement in the surface properties (hydrophilicity) of the zeolite membrane.

7. The ultrafiltration studies have also shown that there is a certain pressure value at which the rejection is optimum. This optimum pressure has been determined by defining an objective function, which is the product of the separation achieved by the membrane and the surfactant flux. The average value of this optimum pressure comes out to be around 40 psi.
8. It has been observed that after modification, the ratio of surfactant to water flux increases. This confirms the enhancement of the hydrophilic behaviour of the membrane after this chemical modification.

References

1. Kitao S., Asaeda M., Gas separation performance of thin porous silica membrane prepared by sol-gel and CVD methods, Proc. 2nd Int. Conf. Inorg. Mem., Key Engineering materials, Vols 61 & 62, Trans Tech Publications, Switzerland, 267-272, 1991.
2. Lin Y. S. and Burggraaf A. J., CVD of solid oxides in porous substrates for ceramic Cheriyan M., Ultrafiltration and Microfiltration handbook, Technomic publishing Co., Lancaster, 1998.
3. Sourirajan S., Reverse Osmosis, Logos press, London, 1970.
4. Hsieh H. P., Inorganic membrane reactors – A review, AIChE Symp. Ser., 85, 268 – 288, 1989.
5. Cuperus F. P., Nijhuis H. H., Applications of membrane technology to food processing, Trends Food Sci.Technology, 4, 277- 286, 1993.
6. P. Meares (Ed.), Membrane Separation Processes, Elsevier, Amsterdam, 1976.
7. Goldsmith R. L., Guest editorial, J. Membrane Sci., 39, 197-201,1988.
8. Gadelle F., Koros W. J., Schechter R. S., Ultrafiltration of surfactant and aromatic/ surfactant solutions using ceramic membranes, Ind. Eng. Chem. Res., 35, 3687-3696, 1996.
9. Dunn R. O., Scamehorn J. F., Christian S. D., Use of Micellar–enhanced ultrafiltration to remove dissolved organics from aqueous streams, Sep. Sci. Technology, 20(4), 257 – 284, 1985.
10. Dunn R. O., Scamehorn J. F., Christian S. D., Concentration Polarization effects in the use of Micellar–Enhanced ultrafiltration to remove dissolved organic pollutants from waste water, Sep. Sci. Technology, 22, 763 – 785, 1987
11. A. Crull, Prospects for the inorganic membrane business, Proc. 2nd Int. conf. on Inorganic membranes, ICIM –91, July 1–4, Montpellier, France, 279, 1991.
12. Geus E.R., Exter M.J.D., Bekkum H.V., Synthesis and characterization of zeolite (MFI) membranes on porous ceramic supports, J. Chem. Soc. Faraday Trans., 88, 3101 – 3109, 1992.
13. Anderson M. A., Gieselmann M. J., Xu Q., Titania and alumina ceramic membranes, J. Membrane Sci., 39, 243 – 258, 1988
14. Niwa M., Ohya H., Tanaka Y., Yoshikawa N., Separation of gaseous mixtures of CO_2 and CH_4 using a composite microporous glass membrane on ceramic tubing, J. Membrane Sci., 39, 301 – 314, 1988.
15. Myatti G. J., Budd P. M., Prince C., Carr S. W., Synthesis of a zeolite NaA membrane, J. Mater. Chem., 2, 1103-111, 1992.
16. Yamazaki S., Tsutsumi K., Synthesis of an A-type zeolite membrane on oxide silicon, Quartz plate and Quartz fiber filter, Microporous Mater., 4, 205-214, 1995.

17. Boudreau L. C., Tsapatis M., A highly oriented thin film of zeolite A, Chem. Mater., 9, 1705-1716, 1997.

18. Aoki K., Kusakabe K., Morooka S., Preparation of oriented A-type zeolite membranes, AIChE Journal, 46(1), 221-224, 2000.

19. Geus E. R., Bakker W. J. W., Verhejien P.J. T., Den Exter M. J., Permeation experiments on in-situ grown ceramic MFI–type films, Proc. 9th Int. Zeolite Conf., Montrell, 371, 1993.

20. Dong J., Dou T., Zhao X., Gao L., Synthesis of membranes of zeolites ZSM-5 and ZSM- 35 by the vapor phase method, J. Chem. Soc., Chem. Commun., 22, 1056-1058, 1992.

21. Yan Y., Tsapatsis M., Gavalas G. R., Davis M. E., Zeolite ZSM-5 membranes grown on porous Al_2O_3, J. Chem. Soc., Chem. Commun., 227–228, 1995.

22. Masuda T., Sato A., Hara H., Kouno M., Harihimoto K., Preparation of a dense ZSM-5 Zeolite film on the outer of an alumina ceramic filter, Appl. Catal., 111, 143-150, 1994.

23. Sano T., Kiyozumi Y., Maeda K., Toba M., Niwa S., Preparation of zeolite film using cellulose moulding, Proc. 9th Int. Zeolite Conf., Montreal II, 239-246, 1993.

24. DenExter M. J., Exploratory study of the synthesis and properties of 6-, 8- and 10- ring tectosilicates and their potential application in zeolite membranes, PhD Thesis, Delft University, The Netherlands, Ch.7, 1996.

25. Nishiyama N., Ueyama K., Matsukata M., Synthesis of FER membrane on an Alumina support and its separation properties, Stud. Surf. Sci. Catal., 105, 2195-2218, 1997.

26. Nishiyama N., Ueyama K., Matsukata M., A Defect free Mordenite membrane synthesized by VPT method, J. Chem. Soc., Chem. Commun., 1967-1968, 1995.

27. Kita H., Inoue T., Asamura H., Tanaka K., Okamoto K., NaY Zeolite membrane for the pervaporation separation of Methanol - Methyl tert-butylether mixtures, J. Chem. Soc., Chem. Commun., 45-47, 1997.

28. Inagaki S., Novel mesoporous materials with a uniform distribution of organic group and inorganic oxides in their frameworks, Journal of American Chemical Society, 121, 9611-9614, 1999.

29. Fricke R., Kosslick H., Lischke G., Richter M., Incorporation of Gallium into Zeolites, Synthesis, Properties and Catalytic Application, Chem. Rev., 100, 2303-2405, 2000.

30. Barrer R. M., Hydrothermal Chemistry of Zeolites, Academic Press, London, 1982.

31. Cheetham A. K., Ferey G., Loiseau T., Open-framework inorganic materials, Angew. Chem. Int. Ed., 38, 3268-3292, 1999.

32. Gues E. R., DenExter M. J., Van Bekkum H., Synthesis and characterization of zeolite (MFI) membranes on porous ceramic supports, J. Chem. Soc., Faraday Trans., 88, 3101-3109, 1992.

33. Bakker W. J. W., Zheng G., Kapteijn F., Makkee M., Moulijn J. A., Single and multicomponent transport through metal supported MFI zeolite membranes, Precision process Technology, Weijnen M. P. C., Eds., Kluwer academic publishers, Amsterdam, 425, 1993.

34. Lixiong Z., Dong J. M., Enze M., Synthesis of SAPO-34 ceramic composite membranes, Stud. Surf. Sci. Catal., 105, 2211- 2219, 1997.

35. Poshusta J. C., Vu T. A., Falconer J. L., Noble R. D., Synthesis and permeation properties of SAPO-34 tubular membranes, Ind. Eng. Chem. Res., 37, 3294, 1998.

36. Sano T., Kiyozuni Y., Kawamura M., Mizukami F., Takaya H., Toida Y., Wantanabe M., Toyoda K., Preparation and characterization of ZSM-5 Zeolite film, Zeolites, 11, 842-845, 1995.

37. Bein T., Brown K., Brinker J., Zeolites, Facts, Figures and Future, ed. Elsevier, Amsterdam, 887, 1989.

38. Davis S. P., Borgestedt E. V. R., Suib S. L., Chem. Mater., 2, 712, 1990.

39. Wenyang Xu, Jinping Li and Jinxiang Dong, Synthesis of zeolite by vapour phase method, Adv. Mater., 3, 442-455, 1991.

40. Tsikoyiannis J. G., Haag W. O., Synthesis and characterization of a pure Zeolite membrane, Zeolites, 12, 126-130, 1992.

41. Matsukata M., Nishiyama N., Ueyama K., J. Chem. Soc., Chem. Commun., 339-340, 1994.

42. Matsukata M., Nishiyama N., Ueyama K., Stud. Surf. Sci. Catal., 84, 1184, 1994.

43. Wenyang X., Jianquan L., Wenyuan L., Huiming C., Bingchang L., Nonaqueous synthesis of ZSM-35 and ZSM-5, Zeolites, 9, 468-473, 1989.

44. Qisheng H., Shouhua F., Ruren X., J. Chem. Soc., Chem. Commun., 1486-1488, 1988.

45. Jia M., Chen B., Noble R. D., Falconer J., Ceramic-zeolite composite membranes and their application for separation of vapour-gas mixtues., J. Membrane Sci., 90, 1-10, 1994.

46. Ma Y. H., Xiang S., Formation of zeolite membranes from sols., Patent PCT/US 9302384, 1993.

47. Ma Y. H., Xiang S., Formation and characterization of zeolite membranes from sols., Abstract, Third International conference on Inorganic membranes, Worcester, MA., July 10-14, 1994.

48. Jia M. D., Peineman K. V., Behling R. D., Ceramic-zeolite composite membranes: Preparation, characterization and gas permeance, J. Membrane Sci., 82, 15-26, 1993.

49. Vroon Z. A. E. P., Keizer K., Verweij H., Bruggraaf A. J., Transport properties of a ceramic thin zeolite MFI membrane, Paper, Third International Conference on Inorganic membranes, Worcester, MA, July 10-14, 1994.

50. Falconer J. L., Tuan V. A., Noble R. D., Alkali free ZSM-5 membranes: Preparation conditions and separation performance, Ind. Eng. Chem. Res., 38, 3635-3646, 1999.

51. Yan Y., Davis M. E., Gavalas G. R., Preparation of zeolite ZSM-5 membranes by in-situ crystallization on porous α-Al_2O_3, Ind. Eng. Chem. Res., 34, 1652-1661, 1995.

52. Gavalas G. R., Mergiris C. E., Sam S. W., Deposition of H_2–permselective SiO_2 films, Chem. Eng. Sci., 44, 1982-1988, 1989.

53. membrane modification, AIChE J., 38, 445-454, 1992.

54. Besmann T. M., Lowden R. A., Sheldon B. W., Stinton D. P., Chemical vapour infiltration, Proc. 11th Int. Conf. CVD, ECS Symp., Vol 90 (12), 482-491,1990.

55. Okubo T., Inoue H., Introduction of specific gas selectivity to porous glass membranes by treatment with tetraethoxysilane, J. Membrane Sci., 42, 109-117, 1989.

56. Miller J. R., Koros W. J., The formation of chemically modified γ-alumina microporous membranes, Sep. Sci. Technol., 25, 1257, 1990.

57. Lin Y. S., Burggraaf A. J., Preparation and characterization of high temperature thermally stable alumina membrane composite, J. Am. Ceram. Soc., 74, 219, 1991.

58. Uhlhorn R. J., Zaspalis V. T., Keizer K., Burggraaf A. J., Synthesis of ceramic membranes, Part II Modification of alumina thin films: reservoir method, J. Mater. Sci., 27, 538, 1992.

59. Ma Y. H., Becker Y. L., Moser W.R., Dixon A. G., Effect of catalyst impregnation on the transport properties of porous alumina membranes, Proc. 2nd Int. Conf. Inorg. Mem., Key Engineering Materials, Vols 61 & 62, Trans Tech Publications, Switzerland, 337-346, 1991.

60. Vasant E. F., Pore size Engineering in zeolites, Wiley and sons, New York, NY, 1990.

61. Niwa M., Murakami Y., CVD zeolites with controlled pore-opening size, J. Phys. Chem. Solids, 50, 487, 1989.

62. Lin Y. S., Fransen P., DeVries K. J., Brinkman H. W., Burggraaf A. J., Experimental study on CVD modification of ceramic membranes, Proc. 11th Int. CVD Conf., ECS Symp. Ser., 90 (12), 539-545, 1990.

63. Lin C. L., Gallaher G. R., Bhave R. R., Flowers D. F., Liu P. K. T., Review on potential improvement of commercial microporous ceramic membrane for gas and liquid separation, 2nd Int. Conf. Inorg. Membrane, Montpellier, France, July 3-6, 1991.

64. Chaufer B., Lucas D., Rabiller-Baudry M., Millesime L., Daufin G., Extraction of α-lactalbumin from whey protein concentrate with modified inorganic membranes, J. Membrane Sci., 148, 1-12, 1998.

65. Guizard C., Ajaka N., Besland M. P., Larbot A., Cot L., Hetropolysiloxane membranes designed for the separation of small molecules, Inorg. Mem. ICIM2-91, Proc. 2nd Int. Conf. Inorg. Mem. ICIM2-91, Trans Tech Publications., Zurich, Switzerland, 537-540, 1991.

66. Reed J. S., Introduction to the Principles of ceramic processing, John Wiley & Sons, 1989.

67. Brunnauer S., Emmett P. H., Teller E., J. Am. Chem. Soc., 60, 309, 1938.

68. Yasuda H., Tsai S. T., Pore size of microporous polymer membranes, J. Appl. Polym. Sci., 18, 805-814, 1974.

69. Gregg S. J., Sing K. S. W., Adsorption, Surface area and porosity, 2nd Edn., Academic press, London, 1982.

70. Jakobs E., Koros W. J., Ceramic membrane characterization via the bubble point technique, J. Membrane Sci., 124, 149-159, 1997.

71. Reimann W., Yeo I., Ultrafiltration of Agricultural waste waters with organic and inorganic membranes, Desalination, 109, 263-267, 1997.

72. Yang H., Kuperman A., Coombs N., Mamiche-Afara S., Ozin G. A., Synthesis of oriented films of mesoporous silica on mica, Nature, 379, 703-704, 1996.

73. Jufu F., Buqiang L., Zihao W., Estimation of fluid-fluid interfacial tensions of multi-component mixtures, Chem. Eng. Sci., 41, 2671, 1986.

74. Wayne R. P., Wilkinson G., Advanced Inorganic Chemistry, 5th Ed., John Wiley & Sons, 320-325, 1992.

75. Warneck P., Chemistry of Natural atmosphere, 1st Ed., Academic Press, Sandiago, 1988.

76. Powder Diffraction file Search manual, Published by International Center for Diffraction Data, Pennsylvania, USA, 1978.

77. Charbit F., Steinchen A., Sadaoui Z., Charbit G., Ultrafiltration of cetyltrimethylammonium bromide solutions, J. Membrane Sci., 133, 1-13, 1997.

78. Chi-Sheng J., Lee En-Hsien., Ultrafiltration of soyabean oil/hexane extract by porous ceramic membranes., J. Membrane Sci., 154, 251-259, 1999.

79. Wei Li, Xien Xu, Separation of acetone/water mixtures by a modified γ-alumina membrane via a new method., J. Membrane Sci., 149, 21-27, 1998.